ANALYSIS OF THE VANE SHEAR TEST

A Thesis Submitted
in Partial Fulfilment of the Requirements
for the Degree of
MASTER OF TECHNOLOGY

By
K. S. RAMA KRISHNA

to the

DEPARTMENT OF CIVIL ENGINEERING
INDIAN INSTITUTE OF TECHNOLOGY KANPUR

JANUARY, 1977

CERTIFICATE

This is to certify that the thesis entitled "Analysis of the Vane Shear Test" by K.S. Rama Krishna is a record of work carried out under my supervision and has not been submitted elsewhere for a degree.

M. R. Madhav

January - 1977.

Dr. M.R. MADHAV
Assistant Professor
Department of Civil Engineering
Indian Institute of Technology
Kanpur.

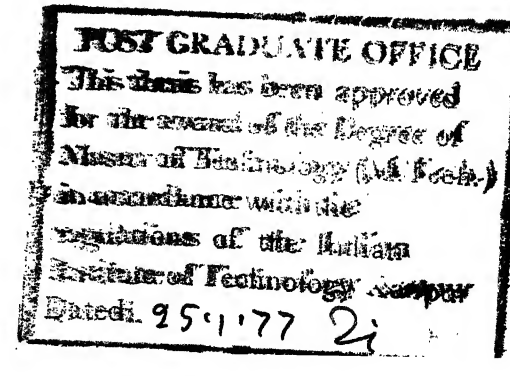

ACKNOWLEDGEMENTS

It gives me great pleasure to express my heartfelt gratitude and sincere thanks to Dr. M.R. Madhav for suggesting the problem and giving invaluable guidance, continuous encouragement and inspiration during the course of the work.

Thanks are due to Messers A. Arumugam, P.P. Vitkar, M.V.S. Rao, R.V. Chalam, N N. Kishore and E.S. Reddy for their kind help during the course of this work.

Thanks are due to Messers K.V. Lakshmidhar, R.P. Trivedi, Gulabchand, Parasu Ram and R.K. Verma for their help in the laboratory.

Finally, I thank Messers V.K. Saxena and G.S. Trivedi for the efficient typing.

K.S. RAMA KRISHNA

SYNOPSIS

of the

Disertation on

ANALYSIS OF THE VANE SHEAR TEST

Submitted in Partial Fulfilment of

the Requirement for the Degree

of

MASTER OF TECHNOLOGY IN CIVIL ENGINEERING

by

K.S. RAMA KRISHNA

Department of Civil Engineering

Indian Institute of Technology, Kanpur

January 1977

Keeping in view, the difficulties involved in securing a reliable, good undisturbed soil sample from the soft soil deposits, and, the advantages and reliability of the vane shear tests over the laboratory tests, two types of analyses of the vane shear test are developed in the present work to evaluate the deformation modulus of the soil.

In the first analysis the normal pressures on the vane blades, at smaller rotations of the vane, are considered.

The analysis is carried out by dividing the vane blade into a number of vertical strips. For more accuracy, the vane blade is further divided into a number of small rectangular elements, thus forming a mesh. This analysis is extended to a square sampling tube, and the influence coefficient obtained. The elasto-plastic analysis is done for square tube and the torque-rotation curve obtained.

In the second analysis, the soil in and around the vane forming a cylinder at a significant amount of the vane rotations is considered. The shear stresses acting on all the three surfaces of the cylinder are considered and an equation for the influence coefficient to measure the soil deformation modulus obtained.

Knowing the linear portion of torque-rotation curve the soil deformation modulus (E_s) can be evaluated from the equation,

$$E_s = \frac{T}{D^3 . \theta . I_\theta}$$

Values of the soil influence coefficients I_θ are derived for different aspect ratios of vane (H/D), different

depth to diameter ratios (H_o/D) and different Poisson's ratios (ν), for the vane (both mechanisms). Similarly, I_θ values are obtained for square tube. Fortunately I_θ values are constant with depth for depths greater than 1.5 to 5.0 diameters. They decrease with increasing Poisson's ratio.

CONTENTS

Page

LIST OF SYMBOLS

B	Side of the square sampling tube
c_u	Undrained cohesion
c_v	Average vane shear strength
D	Diameter of the vane
E_s	Soil deformation modulus
F	A factor in the Hansen and Gibson equation for average vane strength
G	Shear modulus
H	Height of the vane
I_{ij}	Soil displacement influence coefficient
K	Coefficient of Earth pressure at rest
l_G	Length of rectangular portion of Gray's vane
M_c	Resisting moment developed on cylindrical surface
N_c	Bearing capacity factor
p_j	Pressure at the element j
$\{p\}$	Soil pressure vector
q	Cone bearing capacity
$\{r\}$	Radial distance vector
$\{r^*\}$	Dimensionless radial distance vector
R	Radius of vane
s	Shear stress at the equator of the sphere

$[SI]$	Soil displacement influence coefficient matrix
$\{s^{\rho}\}$	Soil displacement vector
S_{α}	Shear strength in the direction with the vertical axis of vane
S_H	Shear strength in the horizontal direction
$S_{U_{(fv)}}$	Field vane undrained strength
S_V	Shear strength in the vertical direction
t	Depth of bottom triangular portion of Gray's vane
T	Torque
T_{max}	Maximum Torque
$\{v^{\rho}\}$	Vane displacement vector
ϕ_f	True angle of internal friction
λ	Compressibility ratio
τ	Shear stress at distance r
τ_o	Shear stress at distance $r = r_o$
γ	Shearing strain at distance r
γ_o	Shearing strain at distance $r = r_o$
ω	Rotation of vane
θ	Rotation of vane
$1^{\rho}{}_{ij}$	Soil displacement at point i of blade 1 due to pressure at element j
ν	Poisson's ratio

LIST OF FIGURES

LIST OF TABLES

CHAPTER 1

INTRODUCTION

In spite of successful efforts to develop techniques intended to minimize the disturbance of sensitive cohesive soils in sampling operation, there exists much evidence indicating that the best of so-called 'undisturbed' samples of many clays do not reveal with desirable accuracy the actual mechanical properties of the various soil layers from which they are extracted. It is generally conceded that the stress changes associated with removal of soil samples from the ground must adversely affect the results of tests made on such samples, and that distortions in the mineral skeleton will introduce relatively important changes in behaviour under stress (Gray 195 High sensitive clays, and the accompanying difficulties in preserving the soil structure, have been encountered chiefly in alluvial (Skempton, 1948), lacustrine (Marsal, 1957) and marine deposits (Gray, 1955 and Flaate 1965), while in many regions mantled by residual soils, the sensitivity of the materials does not appear to be sufficient to warrant much concern with regard to possible sample disturbances.

The undrained shear strength of clay is usually determined in the laboratory on samples taken from different depths in the ground, particularly by unconfined compression test. The shear strength thus obtained increases only slightly with the depth under the soil surface. It is usually smaller than the shear strength calculated from stability analyses, especially in the case of deep sliding surfaces. As mentioned above, this discrepancy may be due partly to the changes in the sample owing to the alteration of pressure conditions during extraction. As this discrepancy is more pronounced at greater depths than at small ones, the latter cause seems to be the more important one (Odenstad, 1948).

These errors, especially that caused by the alteration of pressure conditions, are difficult to eliminate when the shear strength test is carried out on extracted samples. One way would be to re-consolidate the samples to the load that prevailed in the ground, before testing them. Unfortunately this method is rather time-consuming. Still worse, it is not quite reliable, because the sample will acquire a lower pore volume during the reconsolidation and, hence a higher cohesion than it has in the ground (Cadling and Odenstad, 1950). Thus this method is not satisfactory. Another way of avoiding the error is to determine the shear strength directly in the

ground by the vane shear test.

The vane shear tool essentially consists of four thin rigid steel blades rigidly fastened to a centre stem . The top end of the stem is attached to the drill rod which in turn is connected to a torsion equipment. The vane is pushed into the soil gently, and rotated at a constant strain rate with the help of the torsion equipment. The torque-rotation curve is obtained while the test is in progress, and the maximum torque thus obtained is used in the following equation to measure the undrained shear strength (c_u) as,

$$c_u = \frac{T_{max}}{\pi \left(\frac{HD^2}{2} + \frac{HD^3}{6}\right)} \qquad (1.1)$$

Several people developed techniques, to improve the reliability of the vane test results, to measure the strength anisotropy, and to measure the sensitivity of the soils. All this work by different people is reviewed in chapter 2. Cadling and Odenstad (1950) have developed a technique by which it is possible to measure the soil shear modulus (G). This technique is highly inaccurate because of the crude assumptions.

As there exists no reliable method to measure the soil deformation modulus, a technique is developed and presented

in chapter three. Firstly, very small rotations of the vane are considered. At this stage, only the normal pressures on the vane blades will be developed. These pressures are obtained using the condition of compatibility between soil and vane displacements. The normal pressures thus obtained are used to get the torque necessary for this small rotation. Finally, an influence coefficient is obtained with the help of which it is possible to measure the soil deformation modulus in drained as well as undrained condition, once the initial portion of the torque-rotation curve and the diameter of the vane used in a particular test are known.

Each vane blade is divided into a number of vertical strips and the pressure on each vertical strip along the depth of the blade are assumed constant. The equation for the influence coefficient to measure soil deformation modulus is obtained. This technique is extended to the square sampling tube . For more accuracy, each vane blade is further divided into a number of small rectangular elements, thus forming a mesh, and the equation for influence coefficient is obtained.

If a significant amount of rotation is reached while rotating the vane, the soil in and around the vane starts

moving as a cylinder. From this fact, the idea of a cylinder rotating in the soil mass is conceived and a technique developed to measure the soil deformation modulus, which is presented in chapter four.

The shear stresses on the top surface, the bottom surface and the periphery of the cylinder are considered. These stresses are obtained in a similar fashion to those obtained in chapter three. The torque necessary to generate these pressures is also obtained and finally an influence coefficient is given with the help of which it is possible to measure the field soil deformation modulus.

The results of the above analyses for various aspect ratios of the vane and square tube, for various depths and for different Poisson's ratios are presented and discussed and the important conclusions given in chapter five. The equations used to find the soil influence coefficients are given in the appendix. Finally, this thesis ends with a list of references.

CHAPTER 2

REVIEW OF LITERATURE

2.1 Introduction

The vane shear test was developed simultaneously in Sweden by John Olsen in 1928, and in Germany (1929). Little work was done on the vane until 1947, when the Swedish Geotechnical Institute designed several improved vanes and used them on numerous projects. Cadling and Odenstad (1950) published a comprehensive report on this work. About the same time Skempton (1948) in England, designed and used a vane borer and the British Army (1945) designed and used one for testing shallow layers. Since that time a number of publications covering vane testing have appeared, but all have based their actual testing on the original development of the Swedish Geotechnical Institute.

2.2 Measurement of Undrained Cohesion :

2.2.1 Description of vane (Fig.1a) :

Essentially, the vane shear tool consists of four steel blades, rigidly fastened to a centre stem. The top

end of the stem is machined to receive the drill-rod. In order to disturb the soil to be tested as little as possible, the blades must be thin and the stem small in diameter. The apparatus is not intended for use in hard or dense soils.

2.2.2 Testing procedure and advantages :

The shear test in this method is performed by driving a vane into the soil and rotating it, while the resistance to rotation is measured. The undrained shear strength (c_u) is calculated from the maximum torsional moment (T_{max}) thus obtained. The equation relating these two is,

$$T_{max} = \pi c_u \left[\frac{HD^2}{2} + \frac{HD^3}{6}\right] \qquad (2.1)$$

where H and D are the height and diameter of the vane (Fig.2.1). Cadling and Odenstad (1950) introduced some assumptions in the development of the above equation : (i) the surface of rupture is a right circular cylinder having diameter and height equal to those of the vane, (ii) the vane is replaced by a rigid cylinder to which the soil adheres and, therefore, the stress distribution at maximum torque is uniform across the surface of rupture.

With this method, both types of errors mentioned in chapter 1 seem to be practically eliminated. The rotation of the vane requires less time than is usually allowed to elapse between driving and excavation of a sample tube, and also once the vane test has been performed, a saving of time can result from the fact that no sealing, marking and transportation of an undisturbed sample may be necessary nor need an unconfined compression test be performed except to secure comparative data. The real justification for such field vane tests resides in the greater reliability which the results appear to possess.

2.2.3 Further work on vane test :

Skempton (1948) has developed a technique to measure the remolded strength of clay in-situ by the vane test and has stated that, at all depths, the remolded strength as measured by the vane are approximately equal to the values obtained by compression tests. This clearly shows the disadvantages in testing the undisturbed samples. Hansen and Gibson (1949) assuming plane strain conditions and H/D of vane as 1.5, have derived an equation for average vane strength as

$$\frac{c_v}{p} = \frac{K \cos \phi_f + K \sin \phi_f}{1 + \left(\frac{1 - \lambda}{1 + \lambda}\right) \sin \phi_f} \cdot F \qquad (2.2)$$

where, K = Coefficient of earth pressure at rest,

ϕ_f = True angle of internal friction,

λ = Compressibility ratio, and

F = a factor not differing greatly from unity.

Hansen (1950) has conducted vane tests, cone tests, and quick shear tests on Norwegian quick clays, and has found that upto 15 metres depth all these test results agree with one another, and below 15 metres vane tests show substantially higher strengths than the other two. He has stated that the vane tests should very nearly be equal to the minimum strength developed by slides. Kjellman (1950) has conducted many tests on Swedish clays and stated that vane tests are more reliable. Gray (1955) has used a vane which during rotation develops a cylindrical surface and a conical surface at the bottom (Fig 2.1b). Assuming constant shear stress on the cylindrical and conical surfaces, the equation for maximum torque (T_{max}) will be,

$$T_{max} = M_c \left[1 + \sqrt{\frac{R^2 + t^2}{3l}} \right] \qquad (2.3a)$$

and, assuming constant shear stress on cylindrical surface and shear stress on conical surface proportional to the radial distance, the equation for total torque (T) will be,

$$T = M_c \left[1 + \frac{\sqrt{R^2 + t^2}}{4l} \right] \qquad (2.3b)$$

where M_c = Resisting moment developed on cylindrical surface and is given

by $$M_c = \tau_{max} \cdot 2 \pi R^2 l \qquad (2.3c)$$

τ_{max} = Shear stress,

R = Radius of vane, l = length of rectangular portion of blade, and t = depth of conical portion.

Vey (1955) has used two vanes of different lengths and same diameter to investigate the disturbance caused by the insertion of vane into the soil and has found that large vane values are less affected by the insertion because the disturbance is greatest near the centre of the vane. Marsal (1957) has brought out a new design in vane shear test in which the friction on the supports of the rods that connect the vane with the operation platform, is eliminated by measuring the torque at the lower end of the transmission system near the vane by using a torsion cell equipped with strain gauges. He also confirmed the advantages of vane shear test over unconfined compression tests. Sridharan and Madhav (1964) have showed from laboratory vane tests, the

increase in strength, decrease in failure strain and increase in the sensitivity with the rate of rotation. Andersen and Sollie (1965) have designed a light inspection vane for quick and easy measurements of the undrained shear strength of clays, in the field, the range of the instrument being 0 to 20 t/m^2. Hall and Miller (1965), in their tests on 30" long undisturbed samples, have observed the variation of strength from top to bottom. Sibley and Yamane (1965) have developed a hand operated torsional vane shear device which has eight blades. It can be used both in the field and in the laboratory. A calibrated dial is provided on top of the handle which converts the torque into T/ft^2 directly. They have also introduced three vane adapters, one for very soft soils, another for soft soils and the third one for stiff clays. Lo (1970) has suggested that a small vane can be conveniently used to determine the intact strength of fissured clay if the clay is not strongly anisotropic. Koutsoftas, Demetrious and Fisher (1976) have found a relation between in-situ undrained strengths from field vane and cone penetrometer soundings as

$$q_c = (16 \pm 3)\, S_{u(fv)} \qquad (2.4)$$

where q_c = cone bearing capacity,

$S_{u_{(fv)}}$ = field vane undrained strength.

Wilson (1950) has developed an interesting technique to obtain the in-situ shear strength of soil with the help of square sampling tube (Fig 2.1.c). Here the torque-rotation curve is obtained in a similar fashion to the one from vane shear test. This technique has the advantage of measuring in-situ strength and obtaining good undistrubed sample simultaneously. The equation for shear strength given by him, is

$$c_u \approx \frac{6}{21\ B^2\ L} \cdot T \qquad (2.5a)$$

and for a square tube with B = 2" & L = 24",

$$c_u \approx 5.2\ T \quad (T \text{ in ft - lb}) \qquad (2.5b)$$

(L = length of tube in inches, B = width of tube in inches and c_u is in kips per sq.foot)

2.3 Measurement of Strength Anisotropy :

Aas (1965), using vanes with different shapes, has presented a method for approximate determination of the

ratio between the undrained shear strength acting along horizontal (S_H) and vertical (S_V) failure surfaces. He has found the ratio S_H/S_V to be 1.1 in the case of over consolidated clays and between 1.5 and 2.0 in the case of normally consolidated clays. Flaate (1966) has pointed out the necessity of using two or more vanes with different dimensions at each depth of test to separate the horizontal and vertical shear strengths and suggested an equation relating torque at failure (T) to the shear strengths in the horizontal (S_H) and vertical (S_V) directions, as

$$T = \frac{\pi D^3}{6} \left[\frac{3H}{D} S_V + S_H \right] \qquad (2.6)$$

This is similar to the one given by Cadling and Odenstad, when $S_H = S_V$. Madhav and Roy (1970), using rectangular and trapezoidal shaped vane blades, have found a method to determine the shear strength anisotropy of a soil and the undrained cohesion of the clay in any direction. Northwood and Sangrey (1971) have investigated the strength anisotropy of peat with vanes of varying shape and showed that strengths on the vertical plane could be 100% higher than those on the horizontal plane and confirmed the draw back in using conventional vanes to interpret results. Menzies and Mailey (1976) have used diamond-shaped vanes of different

angles to measure the variation of shear strength with direction. If a diamond vane of angle α with the vertical vane axis of rotation is used, then soil will be sheared along a plane of angle α with the vertical direction. Assuming the soil to be orthotropic, they have given an equation for the undrained shear strength (S_α) in the direction α as

$$S_\alpha = S_H + (S_V - S_H) \cos^2\alpha \qquad (2.7)$$

where S_H and S_V are the undrained shear strengths in horizontal and vertical directions respectively. This equation is similar to that used by Lo (1965) to represent the variation with direction of unconfined compression strength of a soft Welland clay. Bhaskaran (1971) has stated that the peculiar feature of the vane in contrast to other methods of shear tests is that here, the particles describe paths of motion in the horizontal plane, and hence the anisotropy indicated is likely to be different from that measured in the plane strain or triaxial tests.

2.4 Measurement of Soil Deformation Modulus :

Cadling and Odenstad (1950) have found a method of calculating Deformation Modulus from the torque-angle of twist relationship. If a cylinder of infinite extent and an elastic

soil mass are assumed it can be shown from considerations of equilibrium and elasticity that the deformation modulus is equal to one half the slope of the initial straight line portion of the shear stress-angle of twist curve. Since the cylinder tested is not infinite, the relationship is not exactly true. They have also shown that for a sphere rotated in an elastic soil mass, the relationship is 1/3 instead of 1/2. The actual relationship, therefore, could be in between, but close to 1/2. Their analysis is carried out in the following way.

In the two-dimensional calculation a rigid cylinder of radius r_o has replaced the vane and is extending throughout the whole of clay layer, in the axial direction (Fig. 2.2a) using elasticity and equation of equilibrium, one gets

$$\tau = \tau_o \frac{r_o^2}{r^2} \qquad (2.8)$$

where τ_o = Shear stress at the surface of the cylinder (i.e. at $r = r_o$),

τ = Shear stress at distance r.

Using modulus of rigidity $G = \frac{\tau}{\gamma}$,

equation 2.8 becomes $\gamma = \frac{r_o^2}{r^2}\gamma_o$ (2.9)

where γ = Shear strain at distance r,

γ_o = Shear strain at $r = r_o$.

The rotation ω (from Fig 2.2b) is obtained as

$$\omega = 1/2 \quad \frac{r_o^2}{r^2}\gamma_o \tag{2.10a}$$

and thus $\omega_o = 1/2\,\gamma_o$ (2.10b)

Finally, using the above equations, one gets,

$$G = \frac{\tau_o}{2\omega_o} \tag{2.11}$$

In the three-dimensional calculation, the vane is replaced by a rigid sphere (Figure 2.2b). A small volume element at the surface of the sphere is considered. Using the equations of equilibrium, assuming small deformations, and satisfying compatibility, the equation for shear modulus G is obtained as

$$G = \frac{s}{3\omega_R} \tag{2.12}$$

where ω_R is the rotation of the sphere, and s = Shear stress at the equator of the sphere.

2.5 Drawbacks in the Vane Test :

Jackobson (1954) has made a theoretical study of the field vane test, the laboratory vane test, and the unconfined compression test and showed that the unconfined compression test gives higher values for the shear strength than the vane test in normally consolidated clays to depths of 10 to 15 metres. This is further confirmed by Flaate (1965). In some investigations, it has been found that vane tests give unexpectedly high values for the shear strength when checked against stability analysis. Golder (1962) and Eden (1965) have found that vane tests in dilatant soils could give erroneous values for the shear strength. This is based on the fact that negative pore water stresses, induced during shear deformation, would temporarily increase the effective stresses and give apparently high values for the shear strength. Eden (1965) has also shown that the vane tests in over consolidated clay are not reliable. Bazzett, Adams and Matyas (1961) have found that the values of vane tests in the fissured sensitive marine clays near Ontario, Canada, have resulted in factors of safety on the unsafe side involving errors as great as 70%. Delory & Salvas (1969) have found that vane tests in Canadian silty clays tended to underestimate the strength required for stability. Flaate (1966) has concluded that neither field

vane nor any other undrained shear strength tests measures a'true shear strength'. He has further stated that the assumption with the vane tests, such as, 'change in original stress conditions and amount of remolding of soil involved have no influence on the vane test results', are not always correct.

Among the shortcomings of the vane are stress concentration at edges, unknown stress conditions in the soil surrounding the vane, blade friction effects (Geuze, 1963), and the unanswered questions concerning the shape of the failure surfaces and the width of the strain zone (Kenney and Landva, 1965). Lodd (1967) has stated that there is a severe rotation of the principal stresses in a vane test. This orientation is likely to be both in the vertical and horizontal failure surfaces and is likely to be highly complex. Kenney and Landva (1965) and Haefeli (1965) have stated that soil resistance against vane shear is very sensitive to rates of strain especially at lower rates of shear. Bjerrum (1973) has stated that an undrained analysis based on conventional vane strength does not lead to a correct estimate of the safety factor for all types of clay. Aas(1976) has stated that for low-plastic Norwegian clays this discrepancy is due to the pronounced anisotropic behaviour of the undrained shear strength. He has also observed that an uncritical use

of the vane strength, when it exceeds a value corresponding to about 0.2 times the effective overburden pressure, leads to an overestimation of the stability conditions and thus to unsafe design.

2.6 Ways to Improve the Reliability of Vane Results :

Flaate (1966) has suggested the following points to improve the reliability of vane test results : The test has to be calibrated to the different types of problems that one deals with, every time the test has to be performed in the same way, the vane should be carefully installed, same delay before the test is started (Preferably not more than five minutes after installation), same rate of strain should be used (0.1 deg/second seems to be satisfactory), the actual vane dimensions should not vary too much (H/D = 2.0 with D $\approx$ 2.5" & H $\approx$ 5" are considered reasonable), the area ratio of the vane should be kept as low as possible (preferably, $\not>$ 15%), the results should be interpreted in the same way every time. He has also suggested the necessity of taking samples from the soil deposit where the vane tests are conducted, because knowing the physical properties will help to study the significance of the vane test in different types of clays. Lory and Salvas (1969) have stressed the importance

of knowledge of past and present in-situ stress conditions to appraise fully the shearing strength obtained. Lo (1970) has suggested that a small vane should be used to measure the intact strength of fissured clay if the clay is not strongly anisotropic. Northwood and Sangrey (1971) have studied the variation of shearing strength with vane size in organic soils and suggested 10 cm as the optimum diameter of vane.

The above review indicates that there exists no method to obtain the undrained modulus from vane test results. A method to estimate the same is developed in the following chapters.

CHAPTER 3

ANALYSIS FOR VANE AND SQUARE TUBE, MECHANISM I-SMALL ROTATIONS

3.1 Introduction:

When a vane is pushed into the soil and torque is applied at a constant strain rate, the vane blades exert normal pressure on the soil very next to them. At the very beginning of rotation of blades, i.e., at very small rotations the soil surrounding the blades will be in elastic state only. Here, the soil displacements and the corresponding vane displacements can be equated to satisfy compatibility and an expression for the normal pressures obtained. Once the normal pressures are obtained, the next step will be to use these to find out the torque necessary for that amount of rotation. The present work is intended to obtain an influence coefficient from which the soil modulus can be obtained, once the torque, rotation and the size of the vane are known. The assumptions in this are:

(i) The soil is homogeneous, isotropic and linearly elastic,

(ii) The vane blades are smooth,

(iii) The normal pressures on the vane blades are constant over the depth.

3.2 Analysis of Vane by Vertical Strips:

Each vane blade(Fig. 3.1) is divided into 'n' number of vertical strips. The pressure over each vertical strip is constant with depth but is a function of the distance from the centre of the vane. That is, pressure on the vertical strip near the vane centre is small and increases towards the edge of the vane blade. Each vertical blade is subdivided into 'm' number of elements, and the number 'm' is so chosen that the pressure on each element is approximated as a concentrated load acting at the centre of the element. The displacements of the centre of each vertical strip of the first blade are considered.

3.2.1 Soil displacements:

The soil displacement ($_1\rho_{ij}$) at the centre of the ith vertical strip due to pressure (p_j) on the jth element on the 1st blade is given by:

$$_1\rho_{ij} = \frac{p_j}{E_s} \; D \; I_{ij} \qquad (3.1)$$

where E_s is the soil deformation modulus, and I_{ij} is the influence coefficient obtained by integrating Mindlin's equations for horizontal displacements due to a concentrated horizontal force beneath the soil surface , D is the

diameter of the vane. The Mindlin's equations are given in the Appendix. The influences of all blades are added up to get the soil displacement of point i, as:

$$ {}_s\rho_{ij} = \frac{p_j D}{E_s} \sum_{k=1}^{N_b} (I_{ij})_k \qquad (3.2) $$

where N_b is number of blades (usually four). It is noted that blade 3 would have pressures and displacements in the opposite directions to those of blade 1. The total displacement of point i due to forces acting on all the m x n elements in each blade, is ${}_s\rho_i$ and is given as:

$$ {}_s\rho_i = \frac{D}{E_s} \sum_{j=1}^{n} SI_{ij}\, p_j \qquad (3.3) $$

The soil displacement vector $\{{}_s\rho\}$ is written as:

$$ \{{}_s\rho\} = \frac{D}{E_s} [SI] \{p\} \qquad (3.4) $$

where $\{{}_s\rho\}$ and $\{p\}$ are column vectors of size n and $[SI]$ is a square matrix of size n.

3.2.2 Vane displacements:

If the vane rotates through a very small angle $\Delta\theta$ the displacements of the points on the blades are:

$$ {}_v\rho_i = r_i \Delta\theta \qquad (\text{for } 1 \leqslant i \leqslant n) \qquad (3.5) $$

where r_i is the radial distance of the point i from the centre of the vane. The vane displacement vector is given as:

$$\{{}_v\rho\} = \{r\}\Delta\theta \qquad (3.6)$$

where $\{{}_v\rho\}$ and $\{r\}$ are column vectors of size n.

3.2.3 Equation for soil deformation modulus(E_s):

The vane displacement vector $\{{}_v\rho\}$ is equated to soil displacement vector $\{{}_s\rho\}$ for compatibility, as:

$$\frac{D}{E_s}\ [SI]\ \{p\} = \{r\}\Delta\theta \qquad (3.7)$$

Solving Eq.(3.7);

$$\{p\} = \frac{E_s}{D}\ [SI]^{-1}\ \{r\}\Delta\theta \qquad (3.8)$$

The torque(T) necessary to generate a rotation of $\Delta\theta$ is,

$$T = 4\int p.dA.r \qquad (3.9)$$

$$T = \frac{E_s\Delta\theta}{D}\left([SI]^{-1}\ \{r\}\right)^T\ \frac{H\ D}{2n}\ \{r\}\ 4 \qquad (3.10)$$

or

$$\frac{T}{E_s\Delta\theta} = \frac{2H}{n}\left([SI]^{-1}\ \{r\}\right)^T\ \{r\} \qquad (3.11)$$

The Influence coefficient, I_θ , is given by ,

$$I = \frac{T}{E_s \Delta\theta D^3} = \frac{2}{n} \frac{H}{D} \left([SI]^{-1} \{r^*\} \right)^T \{r^*\} \qquad (3.12)$$

where $\{r^*\} = \left\{\frac{r}{D}\right\}$, a dimensionless vector.

If in a vane test, the torque T corresponding to a rotation θ from the linear portion of the torque vs rotation curve, is known, the soil modulus, E_s , can be estimated using the known values of I_θ obtained above.

The equation for soil modulus, E_s is :

$$E_s = \frac{T}{I_\theta . D^3 . \theta} \qquad (3.13)$$

3.3 Analysis of Square Tube Sampler:

Wilson (1950) has developed a technique to obtain the in-situ shear strength of soil with the help of a square sampling tube, while sampling is in progress. In this technique, the torque-rotation curve is obtained in a similar fashion to the one from Vane shear test. He has showed that with square tube sampler a good undisturbed sample can be taken. Keeping these advantages in view, the present work is extended to the square tube sampler. The pressures on the soil around the tube are as shown in Fig. 3.2.

The analysis in this case is similar to the analysis of vane, the only difference being in the coordinates. The coordinates of elements of the square tube with reference to those in the analysis by vertical strips (Fig. 3.2) are given below:

Face (2):

$$x = -\left(XP + \frac{D}{2}\right) \qquad (3.14\ a)$$

$$y = \left(\frac{D}{2} - XQ\right) \qquad (3.14\ b)$$

Face (3):

$$x = D \qquad (3.14\ c)$$

$$y = -\left(XP + XQ\right) \qquad (3.14\ d)$$

Face (4):

$$x = XP - \frac{D}{2} \qquad (3.14\ e)$$

$$y = -\left(XQ + 0.5\right) \qquad (3.14\ f)$$

where XP is the distance of points on the vane blade(1) from centre of vane and XQ is the distance of elements on vane blade (1) from centre of vane.

The equation for the soil deformation modulus(E_s) is:

$$E_s = \frac{T}{I_\theta\ B^3\ \theta} = \frac{2}{n}\ \frac{H}{B}\ \left(\left[SI\right]^{-1}\ \{r^*\}\right)^T\ \{r^*\} \qquad (3.15)$$

where B is the side of the square tube, I_θ is the influence

coefficient obtained in the same way as in analysis of vane test by strips, H is the height of the tube, n is the number of vertical strips into which half the side of the tube is divided, $[SI]$ is the soil displacement influence coefficient matrix of size n, r^* is the column vector of the distances of the centres of 1 to n strips from a vertical line dividing the tube side in to two halves and $\frac{T}{\theta}$ is the initial slope (linear portion) of the torque-rotation curve obtained from field vane test.

3.4 Elasto-Plastic Analysis of Square Tube:

As the vane is rotated in the soil medium, at some rotation the pressure on the strip (n) near the edge of the blade reaches yield values. The pressures on the strips from edge towards the centre also reach yield values, gradually, during the progress of rotation of the vane. The stress-strain curve for the soil is shown in Fig.5.5a. The compatibility condition will not be satisfied for elements which yield and slip is expected to occur. The analysis based on elasticity can be done to those strips on which the pressures do not reach yield values.

If the pressure on the nth strip reaches yield value satisfying compatibility for the elements 1 to (n-1),

Eq. 3.7 becomes:

$$\begin{bmatrix} SI_{1,1} & SI_{1,2} & \cdots & SI_{1,n-1} \\ SI_{2,1} & SI_{2,2} & \cdots & SI_{2,n-1} \\ \vdots & & & \vdots \\ SI_{n-1,1} & & \cdots & SI_{n-1,n-1} \end{bmatrix} \begin{Bmatrix} p_1/E_s \\ p_2/E_s \\ \vdots \\ \frac{p_{n-1}}{E_s} \end{Bmatrix} = \begin{Bmatrix} r_1^* \\ r_2^* \\ \vdots \\ r_{n-1}^* \end{Bmatrix} \Delta\theta \qquad (3.16)$$

The pressures, p_1/E_s, p_2/E_s .... $\frac{p_{n-1}}{E_s}$ can be obtained as:

$$\left\{ \frac{p}{E_s \cdot \Delta\theta} \right\} = [SI]^{-1} \{r^*\} \qquad (3.17)$$

Torque (T) needed for generating these pressures will be,

$$\frac{T}{E_s D^3} = \left([SI]^{-1} \{r^*\} \right)^T (A) \{r^*\} \theta + \frac{p_n}{E_s} \theta (A) (r_n) \qquad (3.18)$$

where A is the area of each strip and p_n/E_s is the yield value of pressure at strip $n = \frac{c_u N_c}{E_s D^3}$, c_u = undrained cohesion, N_c=bearing capacity factor = 9 for depth greater than five diameters. Similarly, if the pressures on strips n-2, n-3...n-i reach yield values then the equation for torque will be:

$$T = \sum_{j=1}^{n-i} p_j \cdot \Delta A \cdot r_j + \sum_{j=n-i+1}^{n} \left(\frac{c N_c}{E_s} \right) \Delta A \cdot r_j \qquad (3.19)$$

Thus the torque vs rotation curve can be obtained.

3.5 Analysis of Vane Test by Mesh:

In this analysis the normal pressures on the vane blades are not assumed constant over the depth, and the analysis is carried out in the following way with the

assumptions: (i) the soil is homogeneous, isotropic and linearly elastic and (ii) the vane blades are smooth.

Each vane blade is divided into n parts in each direction, thus making a mesh of n x n rectangular blocks (Fig. 3.3). Each block is subdivided into m x m number of rectangular elements. The normal pressure on each of these elements is approximated as a concentrated force acting at its centre, and the displacements of the centres of all the rectangular blocks in the first blade are considered.

As in the previous analysis, the equation for normal pressure can be obtained. It is given as:

$$\{p\} = \frac{E_s}{D} [SI]^{-1} \{r\} \Delta\theta \qquad (3.19)$$

And, the equation for torque (T) is,

$$T = 4.\int p.dA.r$$

$$= \frac{E_s}{D}\left([SI]^{-1}\{r\}\right)^T \Delta\theta \cdot \frac{H}{n}\frac{D}{2n}\{r\} \quad 4 \qquad (3.20)$$

$$\frac{T}{E_s \Delta\theta} = \frac{2H}{n^2}\left([SI]^{-1}\{r\}\right)^T .\{r\} \qquad (3.21)$$

In dimensionless form,

$$I_\theta = \frac{T}{E_s D^3 \Delta\theta} = \frac{2}{n^2}\frac{H}{D}\left([SI]^{-1}\{r^*\}\right)^T \{r^*\} \qquad (3.22)$$

$$E_s = \frac{T}{I_\theta D^3 \Delta\theta} \qquad (3.23)$$

CHAPTER 4

ANALYSIS FOR VANE, MECHANISM II-CYLINDER

4.1 Introduction:

As the vane is rotated in the soil medium a cylindrical surface starts forming in the soil. In this analysis the vane is replaced by a rigid right circular cylinder of the same diameter and height as those of the vane. Here the pressures are developed on all the three surfaces of the cylinder. The displacements of the cylinder in the angular direction and those of the soil surrounding the cylinder are calculated and equated for compatibility. From these, the equations for pressures on top surface periphery and bottom surface of the cylinder are obtained. Then, these pressures are used to find the torque necessary to generate them. Finally, an equation for the soil deformation modulus is derived .

The assumptions in this analysis are the soil is homogeneous, isotropic and linearly elastic.

4.2 Analysis:

The top and bottom surfaces of the cylinder (Fig.4.1) are divided into 'm' number of annular rings and each ring

is further divided into 'n' number of parts in the circumferential direction. The periphery is divided into 'l' number of rings and each ring is further divided into 'n' number of parts. As shown in Fig. 4.1 the displacements at the centres of each ring are considered.

4.2.1 Displacements:

(a) Top surface of soil adjacent to top surface of cylinder:

(i) Top surface: The centre of any ring is designated by i (Fig. 4.1) and the centre of any element on the top surface is designated by j. The soil displacement of i due to pressure (p_j) on element j is given by:

$$s\rho_{ij} = \frac{p_j}{E_s} .D. I_{ij} \qquad (4.1)$$

and the displacement of i due to all elements in any ring is:

$$s\rho_{ij} = \frac{p_j}{E_s} .D. \sum_{n_i=1}^{n} (I_{ij})_{ni} \qquad (4.2)$$

Then, the displacement of i due to all elements of the top surface is :

$$s\rho_i = \frac{D}{E_s} \sum_{j=1}^{m} \sum_{n_i=1}^{n} (I_{ij})_{ni} \times p_j \qquad (4.3)$$

The soil displacement vector for the points on the top

surface due to all elements of the top surface, is given by:

$$\left\{ {}_s\rho_{TT} \right\} = \frac{D}{E_s} \left[SI_{TT} \right] \left\{ p_T \right\} \qquad (4.4)$$

where $\left[SI_{TT} \right]$ is the soil influence coefficient matrix(m x m) for points 1 to m of top surface due to elements of the top surface, and $\left\{ p_T \right\}$ is a row vector of size m of pressures on top surface.

(ii) Periphery:

Similarly the displacements vector $\left\{ {}_s\rho_{TC} \right\}$ of all points of top surface due to all elements of the periphery is given by:

$$\left\{ {}_s\rho_{TC} \right\} = \frac{D}{E_s} \left[SI_{TC} \right] \left\{ p_C \right\} \qquad (4.5)$$

where SI_{TC} is the soil influence coefficients matrix(m x 1) for points of top surface due to elements of the periphery and p_C is a column vector of size 1, of pressures on periphery.

(iii) Bottom surface:

Similarly the displacements vector $\left\{ {}_s\rho_{TB} \right\}$ of all points of the top surface due to all elements of the bottom surface is given by:

$$\left\{ {}_s\rho_{TB} \right\} = \frac{D}{E_s} \left[SI_{TB} \right] \left\{ p_B \right\} \qquad (4.6)$$

where, $\left[SI_{TB} \right]$ is the soil influence coefficients matrix (m x m) for points of top surface due to elements of the bottom surface, and $\left\{ p_B \right\}$ is a column vector, of size m, of pressures on the rings of the bottom surface.

(b) Rotation of points of the top surface of the cylinder (${}_c\rho_T$):

The rotation of points 1 to m of the top surface of the cylinder is given as:

$$\left\{ {}_c\rho_T \right\} = \left\{ r_T \right\} \Delta\theta \qquad (4.7)$$

Now equating the soil displacements of points of the top surface and the rotations of points of the top surface of cylinder for compatibility:

$$\{r_T\} \cdot \Delta\theta = \frac{D}{E_s}\left(\left[SI_{TT}\right]\{p_T\} + \left[SI_{TC}\right]\{p_C\} + \left[SI_{TB}\right]\{p_B\}\right) \tag{4.8}$$

(c) Periphery:

Working on the same lines, one can obtain the equation of compatibility for points on the periphery, as:

$$\{r_C\}\Delta\theta = \frac{D}{E_s}\left(\left[SI_{CT}\right]\{p_T\} + \left[SI_{CC}\right]\{p_C\} + \left[SI_{CB}\right]\{p_B\}\right) \tag{4.9}$$

where $\left[SI_{CT}\right]$ = soil influence coefficients matrix (1 x m) for points of periphery due to all elements of the top surface,

$\left[SI_{CC}\right]$ = soil influence coefficients matrix(1 x 1) for points of periphery due to all elements of the periphery, and

$\left[SI_{CB}\right]$ = soil influence coefficients matrix (1 x m) for points of periphery due to all elements of the bottom surface , and

$\{r_C\}$ = a column vector of size 1 of the radial distances of points of periphery from the vertical axis of the cylinder.

(d) Bottom surface:

Similarly for points of bottom surface, one can obtain:

$$\{r_B\}\Delta\theta = \frac{D}{E_s}\left[SI_{BT}\right]\{p_T\} + \left[SI_{BC}\right]\{p_C\} + \left[SI_{BB}\right]\{p_C\} \quad (4.10)$$

where, $\left[SI_{BT}\right]$ = soil influence coefficients matrix (m x m) for all points of bottom surface due to all elements of top surface,

$\left[ST_{BC}\right]$ = soil influence coefficients matrix (m x 1) for all points of bottom surface due to all elements of periphery,

$\left[SI_{BB}\right]$ = soil influence coefficients matrix (m x m) for all points of bottom surface due to all elements of bottom surface and

$\{r_B\}$ = a column vector of size m, of the radial distances of the points of bottom surface from the centre of the bottom surface.

4.2.2 Pressures:

Equations 4.7, 4.8 and 4.9 can be combined in the following fashion to solve for pressures $\{p_T\}$, $\{p_C\}$ and $\{p_B\}$:

$$\{R\} \times \Delta\theta = \frac{D}{E_s} \left[A\right] \times \{p\} \quad (4.11)$$

where,

$$\{R\} = \begin{Bmatrix} \{r_T\} \\ \{r_C\} \\ \{r_B\} \end{Bmatrix}$$

$$[A] = \begin{bmatrix} [SI_{TT}] & [SI_{TC}] & [SI_{TB}] \\ [SI_{CT}] & [SI_{CC}] & [SI_{CB}] \\ [SI_{BT}] & [SI_{BC}] & [SI_{BB}] \end{bmatrix}$$

and

$$\{P\} = \begin{Bmatrix} \{p_T\} \\ \{p_C\} \\ \{p_B\} \end{Bmatrix}$$

From equation (4.11), p can be obtained as:

$$\{P\} = \frac{E_s}{D} [A]^{-1} \times \{R\} \qquad (4.12)$$

or

$$\{P\} = \begin{Bmatrix} \{p_T\} \\ \{p_C\} \\ \{p_B\} \end{Bmatrix} = \frac{E_s}{D} [A^*] \times \{R\} \Delta\theta \qquad (4.13)$$

where, $[A^*] = [A]^{-1}$

For convenience, p_T, p_C and p_B can be separated as:

$$\{p_T\} = \frac{E_s}{D} [A_T] \{r_T\} \Delta\theta \qquad (4.14)$$

$$\{p_C\} = \frac{E_s}{D} \quad [A_C] \quad \{r_C\} \Delta\theta \qquad (4.15)$$

$$\{p_B\} = \frac{E_s}{D} \quad [A_B] \quad \{r_B\} \Delta\theta \qquad (4.16)$$

where, $[A_T]$ = first 'm' rows of matrix $[A^*]$,

$[A_C]$ = 'm+1' to 'm+1' rows of matrix $[A^*]$, and

$[A_B]$ = 'm+1' to 'm+1+m' rows of matrix $[A^*]$.

4.2.3 Equation for soil modulus:

Equation for torque (T) necessary to rotate the cylinder by $\Delta\theta$ is given as:

$$T = p \cdot r \, dA$$

$$= \{p_T\}^T \{r_T\} A_T + \{p_C\}^T \{r_C\} A_C + \{p_B\}^T \{r_B\} A_B \qquad (4.17)$$

where, A_T is the area of each ring of top surface, and

$$A_T = \left(\frac{D}{2m}\right) \cdot 2 \cdot r_j \qquad (4.18)$$

$$= \left(\frac{D}{2m}\right) \cdot 2 \cdot \frac{D}{2m} \cdot \left(\frac{2j-1}{2}\right) = \frac{D^2}{4m}(2j-1) \qquad (4.19)$$

where, j = 1 to m,

A_C = area of each ring on periphery, and

$$= \frac{H}{1} \cdot 2\pi \cdot \frac{D}{2} = \frac{\pi DH}{1} \qquad (4.20)$$

(where H is the height of the cylinder),

$$A_B = \text{area of each ring on bottom surface;}$$

$$= \frac{D^2}{4m} (2j-1) \qquad (4.21)$$

where, $j = 1$ to m.

Substituting $\{p_T\}$, $\{p_C\}$ and $\{p_B\}$ thus obtained, the equation for torque (T) can be written as:

$$T = \frac{E_s \cdot \Delta\theta}{D} \left(\left([A_T] \{r_T\} \right)^T \frac{D^2\pi}{4m}(2j-1) \{r_T\} + \left([A_C] \{r_C\} \right)^T \frac{\pi DH}{l} \{r_C\} + \left([A_B] \{r_B\} \right)^T \frac{D^2\pi}{4m}(2j-1) \{r_B\} \right) \qquad (4.22)$$

Non-dimensionalizing the above equation with the diameter of the cylinder (D), the influence coefficient I_θ can be written as:

$$I_\theta = \frac{T}{E_s \cdot D^3 \theta} = \left([A_T] \{r_T^*\} \right)^T \frac{\pi}{4m}(2j-1) \{r_T^*\} + \left([A_C] \{r_C^*\} \right)^T \frac{\pi H}{l\, D} \{r_C^*\} + \left([A_B] \{r_B^*\} \right)^T \frac{\pi}{4m}(2j-1) \times \{r^*_B\} \qquad (4.23)$$

where, $\{r_T^*\} = \left\{\frac{r_T}{D}\right\}$, $\{r_C^*\} = \left\{\frac{r_C}{D}\right\}$, and $\{r_B^*\} = \left\{\frac{r_B^*}{D}\right\}$

If in a vane test, the torque T corresponding to a rotation θ from the linear portion of the torque vs rotation curve, is known, the soil modulus E_s can be estimated using the known

values of I_θ obtained above.

The equation for soil modulus, E_s is :

$$E_s = \frac{T}{I_\theta \; D^3 \theta} \qquad (4.24).$$

CHAPTER 5

RESULTS AND CONCLUSIONS

For all the analyses of chapters three and four, the soil influence coefficients matrix [SI] is obtained by numerical integration of Mindlin's equations , on IBM 7044.

5.1 Mechanism I-Strips:

In the analysis by vertical strips, for accuracy, if $i \neq j$, each vertical strip is divided into m subelements. The number m is sufficiently large (Fig.5.1) to approximate the pressure on each element as an equivalent concentrated force acting at its centre. And, if $i = j$, the soil influence coefficients are evaluated using solutions of Douglos and Davis (1964). The solutions of Donglas and Davis together with the original Mindlin's equations are given in the Appendix at the end. The soil pressures and I_θ are plotted as a function of n, the number of vertical strips. If n is chosen as 20 , an arror of only 3 percent is likely to occur in the calculated values of I_θ . For a given n, m equal to 10 gives sufficiently accurate results. From Fig. 5.2 it is evident that, the pressure distributions for distances less than 0.85 R are independent of n, the number of

elements. The pressures tend to infinity assymptolically as the edge of the vane is reached.

Values of I_θ are calculated for a range of values of H/D , H_o/D and poisson's ratio ν , where, H/D = aspect ratio of vane, H_o/D = dimensionless depth to top of vane. For undrained condition ν = 0.5, but if the test is done slowly, or, under drained conditions, ν could be less than 0.5. The effect of poisson's ratio and the depth of the vane from the surface on I_θ is shown in Fig. 5.3a for H/D = 2.0. It is evident from this figure that, I_θ values are independent of H_o/D ratio for H/D > 2.0. I_θ values decrease with increasing poisson's ratio (ν), the decrease being maximum for ν equal to 0.5.

Values of I_θ for different sizes of the vane i.e., for different H/D ratios, are presented in Fig. 5.3b for ν = 0.0 and ν = 0.5. I_θ values increase with H/D ratio, because, for larger vane size more torque is needed to rotate the vane by the same amount.

For square tube also, I_θ values are calculated for a range of values of H/D , H_o/D and poisson's ratio keeping n equal to 40 and m equal to 10. As in the analysis by vertical strips I_θ values are independent of H_o/D, the

depth of test for $H_o/D > 2.0$. Also , it is observed (Fig. 5.4b) that with increasing poisson's ratio, I_θ values decrease the maximum decrease being for $\nu = 0.5$. Values of I_θ for different tube sizes (H/D = 4.5,6.0, 5,9.0, 12.0) are presented in Fig. 5.4b for $\nu = 0.0$ and 0.5. Here also, I_θ -values increase with H/D ratio.

The elasto-plastic stress-strain relation is embedded in the analysis and the nonlinear torque-rotation is obtained as shown in Fig. 5.5a, considering yielding of the soil. If the normal pressure on any element reaches the limiting value of cN_c, the soil element yields and slip is assumed to take place. Torque-rotation curves are obtained for $c_u/E_s = 0.01$ and for $H_o/D > 5$, N_c is assumed to be equal to 9. The curves are independent of the depth effect, for depths > 5 diameters. The pressure with distance from the reference vertical line are as shown in Fig. 5.5b for different rotations (θ).

5.2 Mechanism I-Mesh:

In the relatively more accurate analysis by mesh, I_θ values are obtained in the same manner as in the analysis by strips, and the values of I_θ for different poisson's ratio ν , and for different vane sizes, at H_o/D ratios ranging

from 1 to 100, are compared with those from the analysis by strips in Fig. 5.3.

I_θ values from mesh, for H/D equal to 2.0 , are more and for H/D equal to 0.5 and 1.0 are less than those from the strips. This is because the assumption(iii) of Chapter 3, the pressures along the depth of the vane are constant, is not true for larger H/D ratios. For small H/D ratios the assumption will hold good. The pressure variation with depth is shown in Fig.5.5b før mesh and the pressure values from strips are plotted in the same figure. However, I_θ values obtained by the two methods differ only by less than 5 percent.

5.3 Mechamism II-Cylinder:

In this analysis, the soil influence coefficient matrices $[SI_{TT}]$, $[SI_{TC}]$, etc., are evaluated by numerical integration of Mindlin's equations. The Mindlin's equations are given in Appendix. The points, where the displacements are considered, are chosen for convenience along a radial line, on the top and the bottom surfaces, and on the periphery, along a vertical line joining the ends of the top and bottom radial lines.

Variation of pressures on the top and bottom surfaces, and on the periphery are shown in Fig. 5.7. The pressures on the top and the bottom surfaces increase with increasing distance from the vertical axis of the cylinder. On the periphery, the pressures near the top and bottom edges increase assymptotically, and those in the middle portion of the periphery, are almost constant. It is observed that the pressures on the periphery are larger than on flat surfaces and yielding may start near the edges of the periphery.

The effect of poisson's ratio, ν , and the depth of the vane from the surface on I_θ is shown in Fig. 5.8 , for $H/D = 2.0$. For all values of ν , I_θ is independent of H_o/D when $H_o/D > 2.0$. The torque per unit length for cylindrical piles of various non-dimensionalized lengths (L/D) are obtained from the investigations of Poulos (1975) and are given in Table 5.1. It is evident from this table that, the torque/unit length of cylindrical pile is constant for $L/D > 5$. The coefficient I_θ of Poulos (1975) is related to I_θ by the equation $I_\theta = 1/I_\theta(1+\nu)$ 2 .

Table 5.1

L/D	0.25	0.5	0.7	1.0	4.0	5.0	10.0	20	30	50	100
$\frac{1}{I_\phi \cdot L/D}$	6.4	5.56	4.6	4.17	3.68	3.51	3.34	3.34	3.34	3.23	3.23

When torque per unit length is constant, I_θ values will also be constant with depth. It is also observed from the present analysis that, at shallow depths (i.e. for $H_o/D < 2.0$), the pressures on the top surface of the cylinder are very small. As the depth of embedment increases the pressures on the top surface become equal to those on the bottom surface. This is the reason for the low values of I at $H_o/D < 2.0$.

The pressures at the base and at the periphery of a cylindrical pile subjected to torsion, are given by Poulos (1975). The stresses on the corresponding surface from the present analysis are compared with those given by Poulos in Fig.(5.7) and found that both are in close agreement. The slight differences are due to the fact that Poulos(1975) analysed a pile, the top surface of which is free from stresses where as in the present analysis the effect of top surface is also taken into account.

5.4 Comparison of the Two Mechanisms:

I_θ values in the present analysis are higher than those obtained by strips and mesh (Table 5.2). This is because the normal pressures on the vane blade are small compared to the shear stresses on the periphery of the cylinder. Therefore, the torque needed will be less in the

case of strips or mesh and hence I_θ .

Table 5.2

Comparison of I_θ Values from Mesh and Cylinder

H/D	ν	I_θ from Mesh	I_θ from Cylinder
0.5	0.00	0.7077	1.9871
0.5	0.50	0.6268	1.6682
1.0	0.00	1.1529	2.9965
1.0	0.50	1.0000	2.6034
2.0	0.00	2.0134	4.7244
2.0	0.50	1.7210	4.1846

5.5 Conclusions:

The following conclusions are made:

(1-) Knowing the linear portion of the torque-rotation curve and the diameter of the vane in a particular test the soil deformation modulus can be obtained using the equation,

$$E_s = \frac{T}{D^3 . 0 . I_\theta}$$

(2) I_θ values obtained in the two analyses seem to be constant with depth (H_o/D) for H_o/D ratios greater than 2.

(3) I_θ values increase with increasing H/D ratio.

(4) I_θ values decrease with increasing poissons ratio.

(5) The variation of normal and shear stresses with radial distance and depth, respectively is evaluated. The stresses are nearly constant with depth, and increase with radial distance tending to infinity near the edge of the vane blade.

(6) The square tube can also be used to determine the soil deformation modulus, using the I_θ values obtained in this thesis.

REFERENCES

1. Aas, G., 1965. "A Study of the Effect of Vane Shape and Rate of Strain on the Measured Values of In-Situ Shear Strength of Clays," Proc. 6th Inter. Conf. Soil Mech. Found. Eng. (Montreal), pp. 141-145.

2. Aas, G., 1976. "Stability of Slurry Trench Excavations in Soft Clay," Norwegian Geotechnical Institute Publication No.111, Contributions to the Sixth European Conference on SMFE, Vienna 1976, pp. 1-7.

3. Andersen, A., and S. Sollie, 1965. "An Inspection Vane," Vane Shear and Cone Penetration Resistance Testing of In-Situ Soils, A Symposium Presented at the Fifth Pacific Area National Meeting, ASTM, Seattle, Washington, ASTMSTP No. 399, pp. 3-7.

4. Bazett, D.J., Adams, and Matyas, 1961. "An Investigation of Slides in a Test Trench Excavated in Fissured Sensitive Marine Clay," Proc. 5th Int. Conf. Soil Mech. and Found. Eng. (Paris) Vol.1, p 431.

5. Bhaskaran, R., 1971. Discussion on "Anisotropy of a Bentonite Clay by Vane Shear Tests," by Madhav, M.R., and Roy,M.B. 1970 Indian Society of Soil Mech. and Found. Eng.- Indian Geotechnical Journal, Vol.I, pp.226-230.

6. Cadling, L., and S. Odenstad, 1950. "The Vane Borer: An Apparatus for Determining the Shear Strength of Clay Soils Directly in the Ground," Royal Swedish Geotechnical Institute Proceedings 2.

7. Carlson, L., 1948 . "Determination In-Situ of the Shear Strength of Undisturbed Clay by Means of a Rotating Auger," Proceedings, 2nd Int. Conf. on Soil Mech. and Found. Eng. (Rotterdam), Vol. 1, pp. 265-270.

8. Douglas, D.I., and E.H. Davis, 1964. "The Movement of Buried Footings due to Moment and Horizontal Load and the Movement of Anchor Plates," Geotechnique, Vol. 14, No.2, pp.115-131.

9 . Eden, W.J., and J.J. Hamilton, 1957. "The Use of a Field Vane Apparatus in Sensitive Clay," Symposium on Vane Shear Testing of Soils, ASTM STP 193, pp. 41-53.

10. Eden, W.J., 1965. "An Evaluation of the Field Vane Test in Sensitive Clay," Vane Shear and Cone Penetration Resistance Testing of In-Situ Soils, Asymposium Presented at the Fifth Pacific Area National Meeting, ASTM, Seattle, Washington, ASTM STP 399, pp. 8-17.

11. Fenske, C.W., 1957. "Deep Vane Tests in the Gulf of Mexico ASTM STP193, pp. 16-25.

12. Flaate, K., 1966. "Factors Influencing the Results of Vane Tests," Canadian Geotechnical Journal, Feb. 1966, Vol.III, No.1, pp. 18-31.

13. Geuze, E.C.W.A., 1963. Discussion on "Laboratory Vane Tests and the Influence of Pore Water Stresses," Laboratory Shear Testing of Soils, ASTM STP-361, pp. 388-389.

14. Gibbs, H.J., 1957. "An Apparatus and Method of Vane Testing of Soils," Symposium on Vane Shear Testing of Soils, ASTM STP 193, pp. 9-15.

15. Golder, H.Q., 1962. "Techniques of Field Measurement and Sampling ,"Proceedings, 5th Int. Conf. on Soil Mech. and Found. Eng.(Paris) Vol.III.

16. Gray, Hamilton, 1955. "Field Vane Shear Tests of Sensitive Cohesive Soils," Proceedings ASCE, Soil Mech. and Found. Div. Paper No. 755, pp. 1-17.

17. Haefeli, R., 1965. Discussion on "Vane Triaxial Apparatus," Proceedings 6th Int. Conf. on Soil Mech. and Found.Eng. (Canada) Vol.3, p. 326.

18. Hall, E.B., 1964. "Shear-Strength Determination of Soft Clayey Soil by Field and Laboratory Methods," Symposium on Soil Exploration, ASTM STP 351, pp. 53-59.

19. Hall,E.B., and E.A. Miller,1965."A Comparison of Soil Shear Strengths as Determined with Field and Laboratory Vane Shear Apparatus," Vane Shear and Cone Penetration Resistance Testing of In-Situ Soils-A Symposium Presented at the 5th Pacific Area National Meeting,ASTM,Seattle, Washington, ASTM STP 399,pp.18-28.

20. Hansen,J.B.,and R.E. Gibson,1949."Undrained Shear Strength of Anisotropically Consolidated Clays," Geotechnique, Vol.1, pp.189-204.

21. Hansen,J.B., 1950. "Vane Tests in a Norwegian Quick Clay," Geotechnique, Vol.2, pp. 58-63.

22. Hill,W.C.,1957. "Vane In-Place Soil Shear Device Developed and Applied by Oregon State Highway Department," Symposium on Vane Shear Testing of Soils,ASTM STP193,pp.26-40.

23. Jackobsen, B.,1954. "Influence of Sampler Type and Testing Method on Shear Strength of Clay Samples," Royal Swedish Geotechnical Institute, Proc.8.

24. Kallstenius,T.,1957. "Swedish Vane Borer Design," Symposium on Vane Shear Testing of Soils, ASTM STP193,pp.60-63.

25. Kjellman,W.,1950. "Testing the Shear Strength of Clay in Sweden," Geotechnique, Vol.II,No.3,pp.225-231.

26. Koutsoftas, Demetrious, and Joseph A.Fisher,1976. "In-Situ Undrained Shear Strength of Two Marine Clays," Journal of the Geotechnical Eng. Division, ASCE, Vol.102, No. GT9, pp.989-1005.

27. Ladd, C.C., 1964. "Stress-Strain Modulus of Clay in Undrained Shear," Journal Soil Mech. and Found. Div. ASCE 90, SM5, pp. 103-132.

28. Liu, T.K., and T.H. Thornburn, 1963. "Investigation of Surficial Soils by Field Vane Test ,"Symposium on Soil Exploration, ASTM STP351, pp.44-52.

29. Lo,K.Y.,1965. "Stability of Slopes in Anisotropic Soils ," J.of Soil Mech. and Found. Div.,ASCE, Vol.91,SM4,pp.85-106.

30. Lo,K.Y.,1970."The Operational Strength of Fissured Clays," Geotechnique, Vol.20, No.1, pp.57-74.

31. Lory, F.A., and R.J. Salvas, 1969. "Some Observations on the Undrained Shearing Strength Used to Analyze a Failure," Canadian Geotechnical Journal, Vol.6,pp. 97-110.

32. Madhav, M.R.& M.B.Roy, 1970. "Anisotropy of a Bentonite Clay by Vane Shear Test ,"The Journal of Indian National Society of Soil Mech. and Found. Eng.,Vol.9,No.3, pp. 333-340.

33. Marsal, R.J.,1957. "Unconfined Compression and Vane Shear Tests in Volcanic Lacustrine Clays," Conf. on Soils for Eng. Purposes, ASTM STP, pp. 229-241.

34. Merizies, B.K.& L.K.Mailey,1976 ."Some Measurements of Strength Anisotropy in Soft Clays Using Diamond Shaped Shear Vanes ," Technical Note,Geotechnique, Vol.26,No.3, Sept. 1976, pp. 535-538.

35. Mindlin, R.D., 1936. "Force at a Point in the Interior of a Semi-infinite Solid," Physics, Vol.7, pp.195-202.

36. Northwood, R.P.& D.A.Sangrey, 1971. "The Vane Tests in Organic Soils," Canadian Geotechnical Journal, Vol.8, pp. 69-76.

37. Odenstad, Sten, 1948, "Loading Tests on Clay," Proc. 2nd Int. Conf. Soil Mech. and Found.Eng., Vol.1, pp.299-303.

38. Osterberg, J.O., 1957 Introduction to Symposium on"In-Place Shear Testing of Soil by the Vane Method," ASTMSTP, Vol.193, pp.1-7.

39. Poulos, H.G., and E.H. Davis, 1974, Elastic Solutions for Soil and Rock Mechanics, John Wiley and Sons, Inc. pp. 16-19.

40. Poulos, H.G., 1975 "Torsional Response of Piles The University of Sydney, School of Civil Eng. Research Report No. R 264.

41. Sibley, E.A., and George Yamane, 1965. "A Simple Shear Test," Vane Shear and Cone Penetration Resistance of In-Situ Soils, A Symposium Presented at the V Pacific Area National Meating, Seattle, Washington, ASTMSTP399, pp. 39-47.

42. Skempton,A.W., 1948 . "Vane Tests in the Alluvial Plain of the River Forth near Grangemaith ," Geotechnique Vol. 1, pp.111-129.

43. Sridharan, A., and M.R. Madhav, 1964 . "Time Effects on Vane Shear Strength and Sensitivity of Clay ," ASTM, Proceedings, Vol.64, pp. 957-967.

44. Terzaghi,K. 1941 . "Undisturbed Clay Samples and Undisturbed Clay ," Journ.Boston Soc. C.E. Vol.28,p.211.

45. Vey,E. 1955. Discussion on "Field Vane Shear Tests of Sensitive Cohesive Soils," by Gray, Proc. ASCE81, Paper 843, pp.17-20.

46. Wilson,G., 1970. "The Square Tube in Subsurface Exploration", Insitu Investigation in Soils and Rocks," Proceedings of the Conference Organized by the British Geotechnical Society in London 13-15 May 1969,pp.135-143.

47. Wilson, Nyal E., 1963. "Laboratory Vane Shear Tests and the Influence of Pore Water Stresses," Laboratory Shear Testing of Soils, ASTM STP 361,pp.377-389.

APPENDIX

1. Mindlin's Equations:

Horizontal point load Q acting beneath the surface of a semi-infinite mass (Mindlin , 1936).

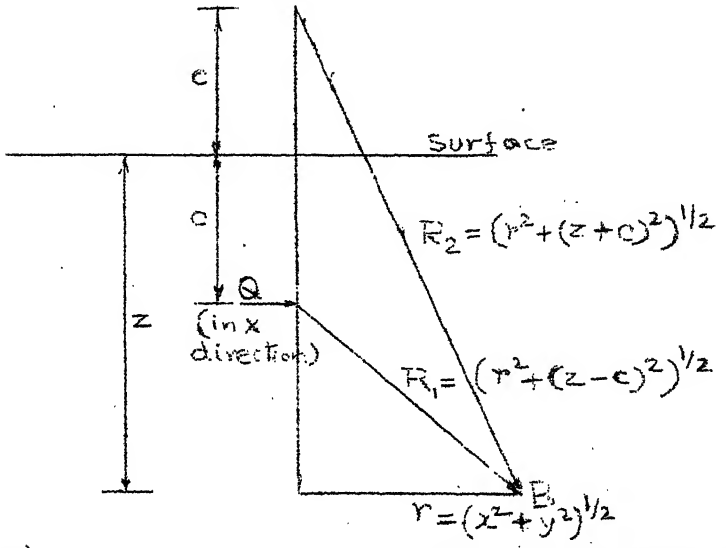

Fig.(A): Horizontal Point Load Acting Beneath the Surface of a Semi-Infinite Mass.

Displacement of B (Fig.A) in the x direction (ρ_x) is:

$$\rho_x = \frac{Q}{16\pi G(1-\nu)}\left[\frac{(3-4\nu)}{R_1}+\frac{1}{R_2}+\frac{x^2}{R_1^3}+\frac{(3-4\nu)\,x^2}{R_2^3}+\frac{2CZ}{R_2^3}\left(1-\frac{3x^2}{R_2^2}\right)+\frac{4(1-\nu)(1-2\nu)}{R_2+Z+C}\,x\left(1-\frac{x^2}{R_2(R_2+Z+C)}\right)\right] \quad (1)$$

Displacement of B in the y direction is:

$$\rho_y = \frac{Q\,xy}{16\pi G(1-\nu)}\left[\frac{1}{R_1^3}\,\frac{(3-4\nu)}{R_2^3}-\frac{6CZ}{R_2^5}\,\frac{4(1-\nu)(1-2\nu)}{R_2(R_2+Z+C)^2}\right] \quad (2)$$

2. Equation Given by Douglas and Davis (1964):

The horizontal displacement of any point of a vertical plane when a rectangular area with the plane is subjected to uniform normal loading (Figure below) is given in the following equations:

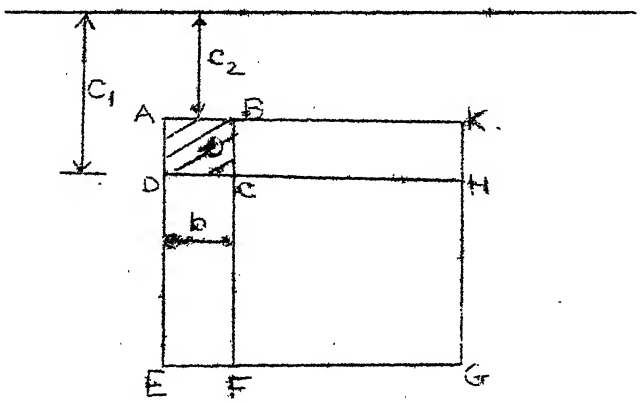

Fig.(B): Co-ordinate System for Uniformly Loaded Rectangles

u_1 and u_2 are the displacements of the bottom and top corner respectively of the rectangle ABCD of Fig. B.

$$u_1 = \frac{pb}{32\ G(1-\nu)} \left\{ (3-4\nu)\ F_1 + F_2 + 4(1-\nu)(1-2\nu)\ F_3 \right\} \quad (3)$$

and

$$u_2 = \frac{pb}{32\ G\ (1-\nu)} \left\{ (3-4\nu)\ F_1 + F_4 + 4\ (1-\nu)(1-2\nu)\ F_5 \right\} \quad (4)$$

where p is the uniform pressure distributed are the shaded area ABCD :

Putting $K_1 = \frac{2\ c_1}{b}$ and $K_2 = \frac{2\ c_2}{b}$

$$F_1 = -(K_1-K_2)\log\left(\frac{(K_1-K_2)}{2+\sqrt{4+(K_1-K_2)^2}}\right)-2\log\left(\frac{2}{(K_1-K_2)+\sqrt{4+(K_1-K_2)^2}}\right) \quad (5)$$

$$F_2 = 2\log\left(\frac{2(K_1+\sqrt{1+K_1^2})}{(K_1+K_2)+\sqrt{4+(K_1+K_2)^2}}\right)+(K_1-K_2)\log\left(\frac{2+\sqrt{4+(K_1+K_2)^2}}{(K_1+K_2)}\right)$$

$$-K_1^2\left(\frac{4+(K_1+K_2)^2}{(K_1+K_2)}-\frac{\sqrt{1+K_1^2}}{K_1}\right) \quad (6)$$

$$F_3 = -2K_1\log\left(\frac{K_1}{1+\sqrt{1+K_1^2}}\right)+(K_1+K_2)\log\left(\frac{(K_1+K_2)}{2+\sqrt{4+(K_1+K_2)^2}}\right)$$

$$-\log\left(\frac{(K_1+K_2)+\sqrt{4+(K_1+K_2)^2}}{2(K_1+\sqrt{1+K_1^2}}\right)+\frac{(K_1+K_2)}{4}\times$$

$$\left[\sqrt{4+(K_1+K_2)^2}-(K_1+K_2)\right]-K_1(\sqrt{1+K_1^2}-K_1) \quad (7)$$

$$F_4 = -2\log\left(\frac{2(K_2+\sqrt{1+K_2^2})}{(K_1+K_2)+\sqrt{4+(K_1+K_2)^2}}\right)+(K_1-K_2)\log\left(\frac{2+\sqrt{4+(K_1+K_2)^2}}{(K_1+K_2)}\right)$$

$$+K_2^2\left(\frac{\sqrt{4+(K_1+K_2)^2}}{(K_1+K_2)}-\frac{\sqrt{1+K_2^2}}{K_2}\right) \quad (8)$$

$$F_5 = 2K_2 \log\left(\frac{K_2}{1+\sqrt{1+K_2^2}}\right) - (K_1+K_2)\log\left(\frac{K_1+K_2}{2+\sqrt{4+(K_1+K_2)^2}}\right)$$

$$+ \log\left(\frac{(K_1+K_2)+\sqrt{4+(K_1+K_2)^2}}{2(K_2+\sqrt{1+K_2^2})}\right) - \left(\frac{K_1+K_2}{4}\right)\times$$

$$\left[\sqrt{4+(K_1+K_2)^2} - (K_1+K_2)\right] - K_2\,(K_2-\sqrt{1+K_2^2}) \qquad (9)$$

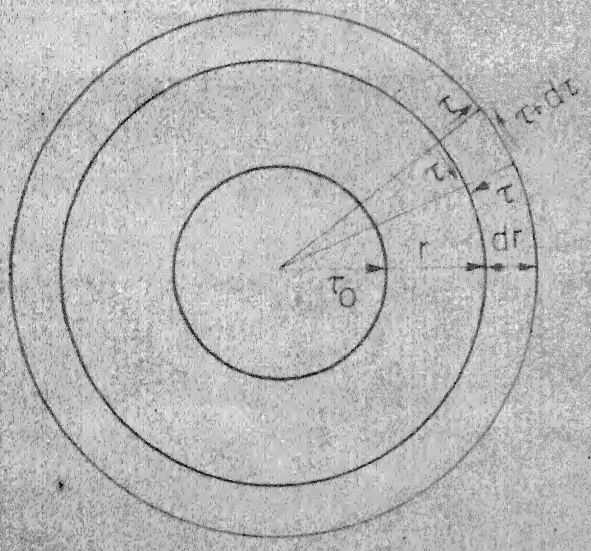

TWO DIMENSIONAL CASE

FIG.2.2a1 SHEARING STRESSES ACTING ON THE ELEMENT UNDER CONSIDERATION

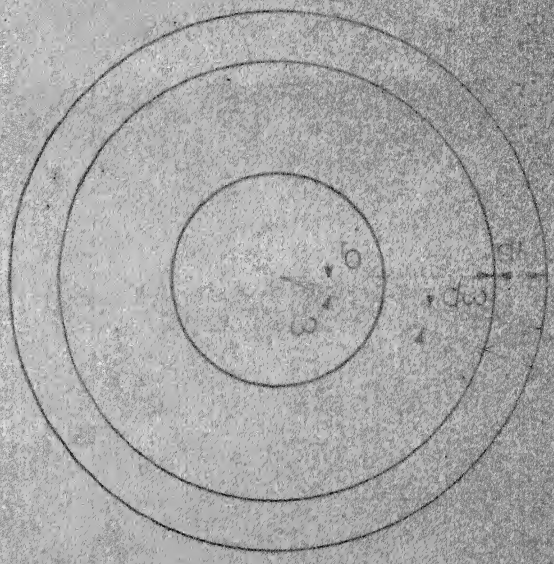

FIG.2.2a2 DEFORMATION OF THE ELEMENT SURROUNDING THE POINT

THREE DIMENSIONAL CASE

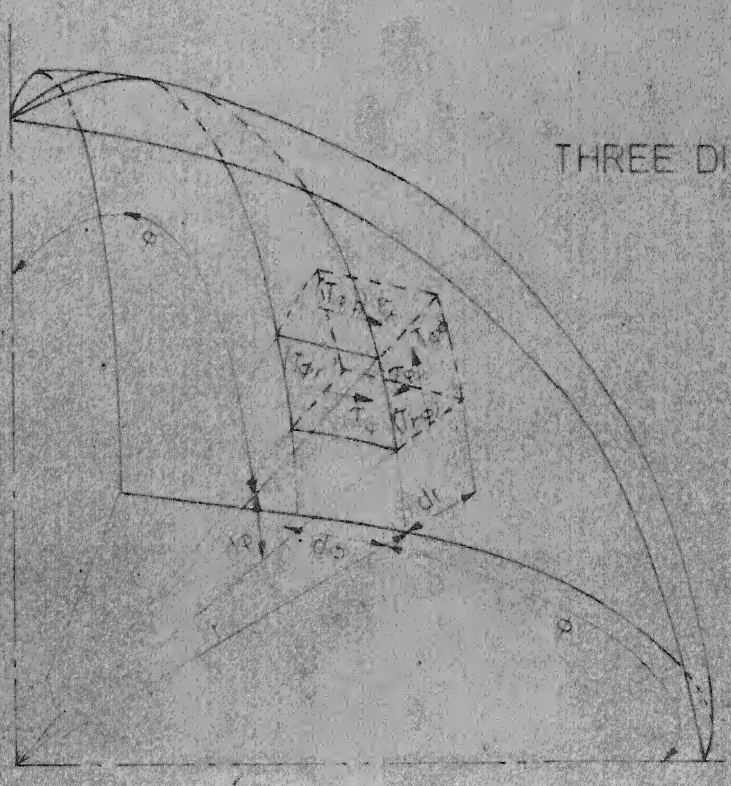

FIG.2.2b SHEARING STRESSES AND FORCES ACTING ON THE ELEMENT

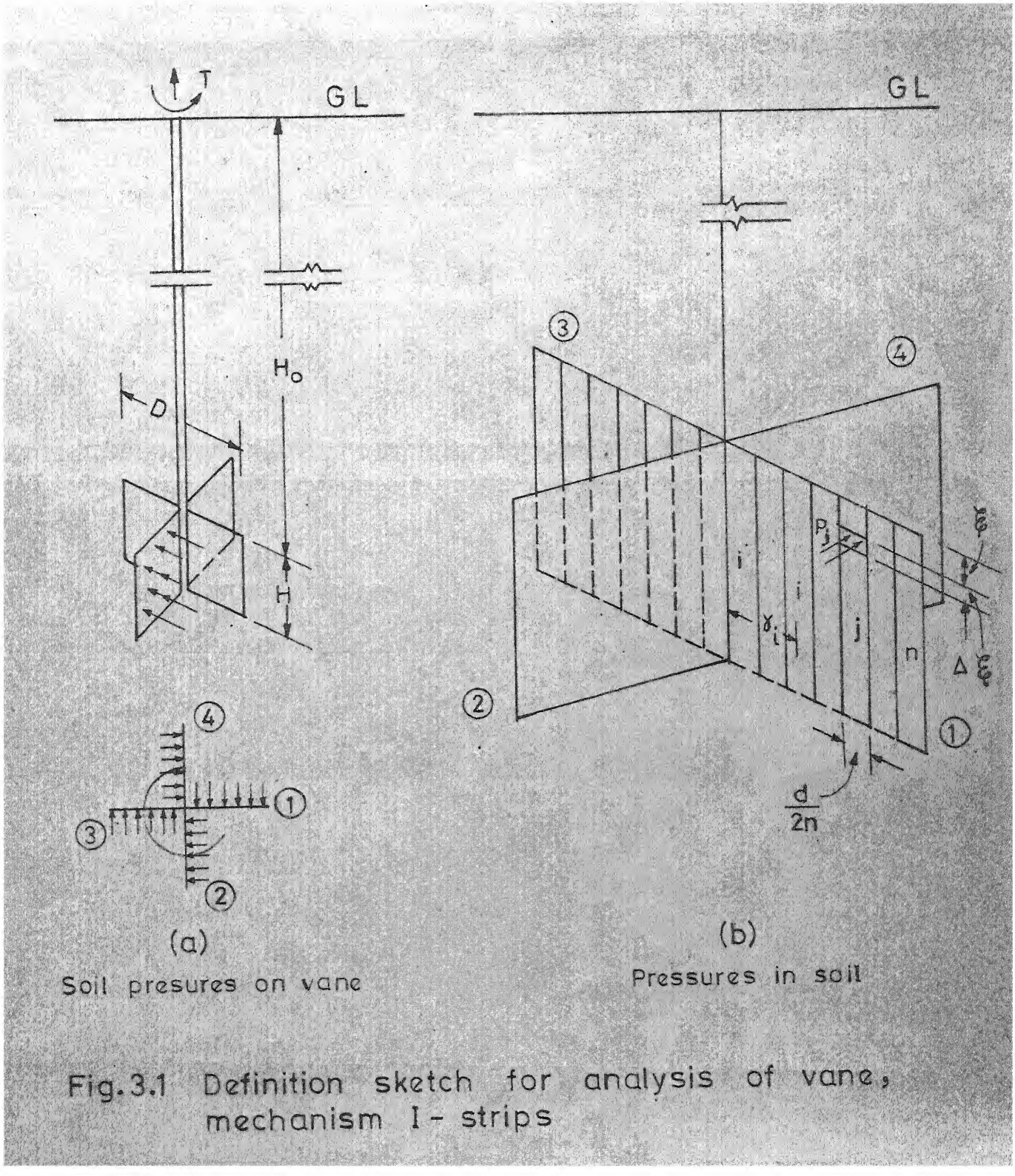

Fig. 3.1 Definition sketch for analysis of vane, mechanism I - strips

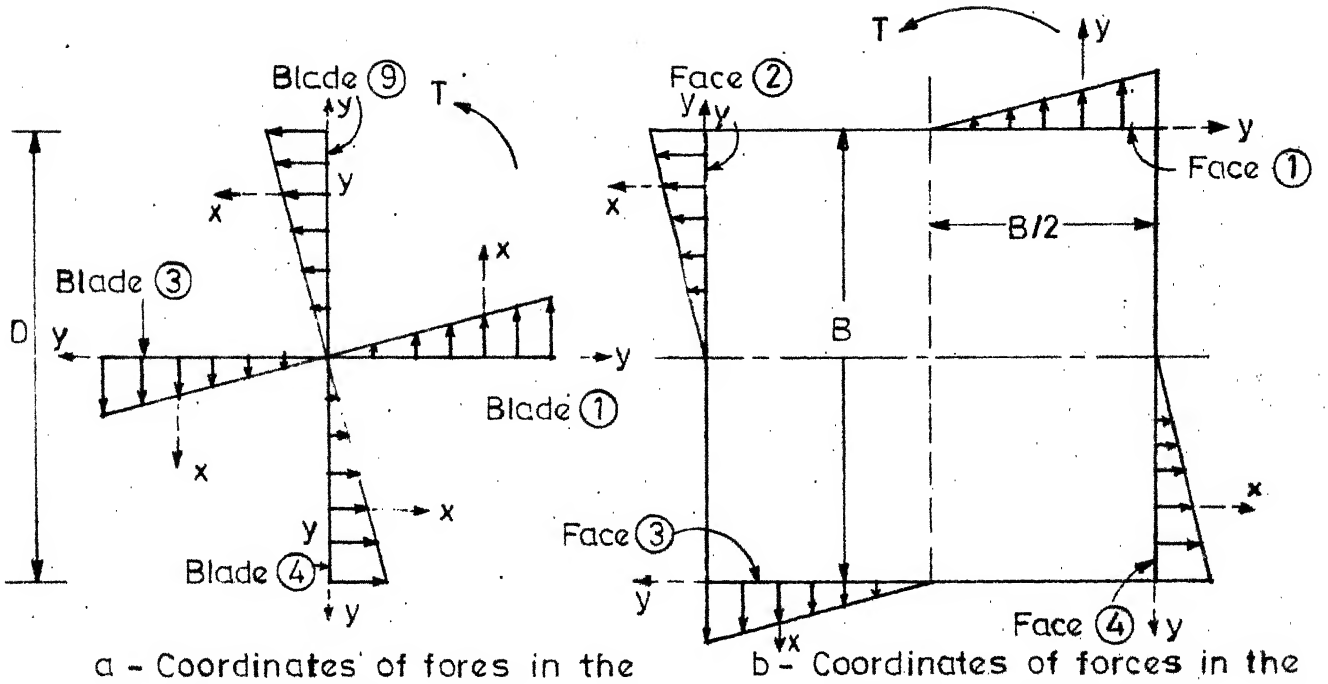

a - Coordinates of fores in the case of vane

b - Coordinates of forces in the case of square tube

Fig.3.2 Definition sketch for square tube related to vane

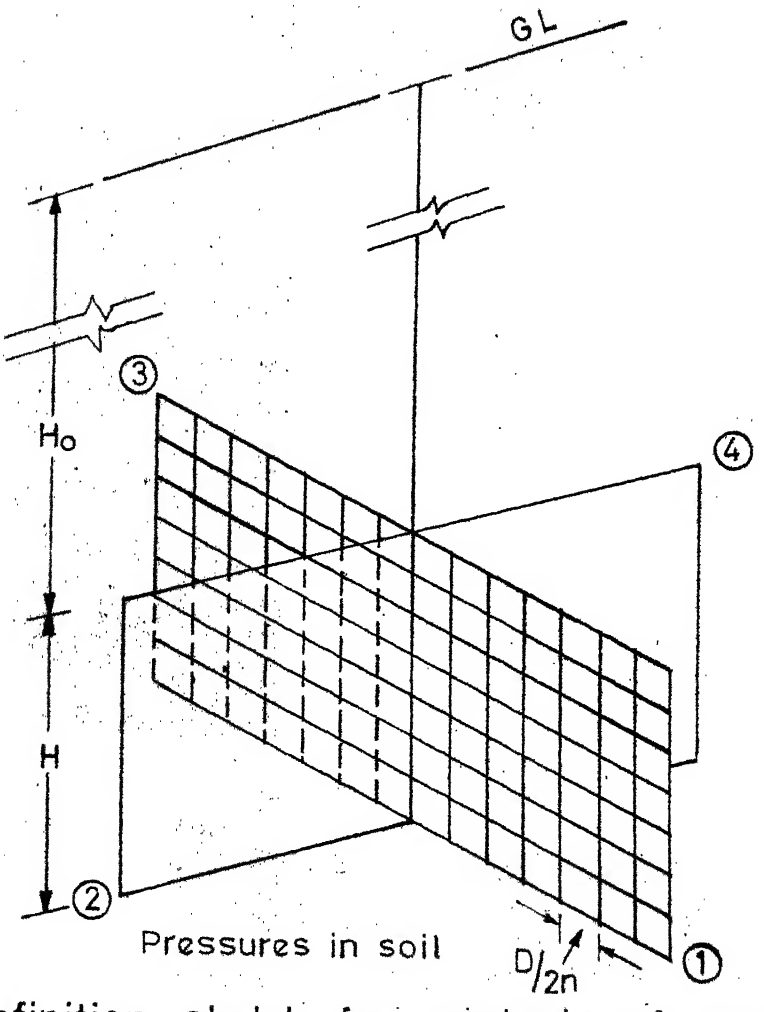

Fig.3.3 Definition sketch for analysis of vane, mechanism I-mesh

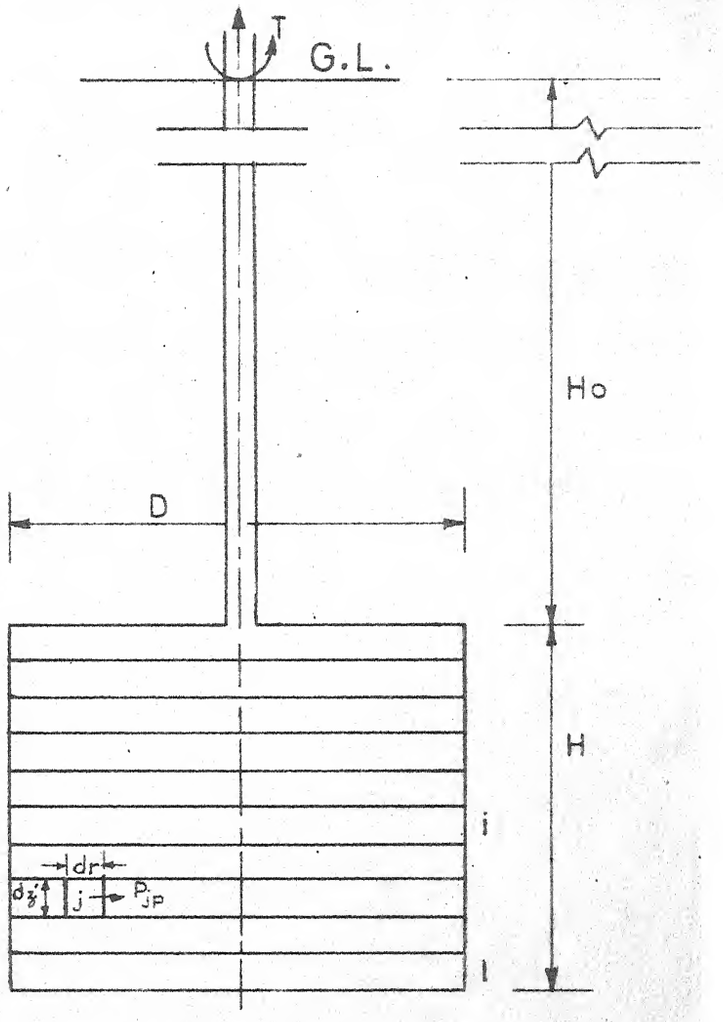

(b) Stresses in soil on the periphery

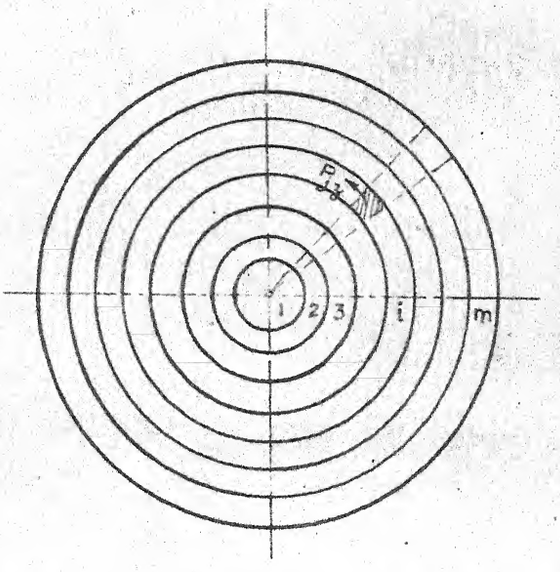

(a) Stresses in soil on top & bottom surfaces

Fig. 4.1 Definition sketch for analysis of vane, mechanism II - cylinder.

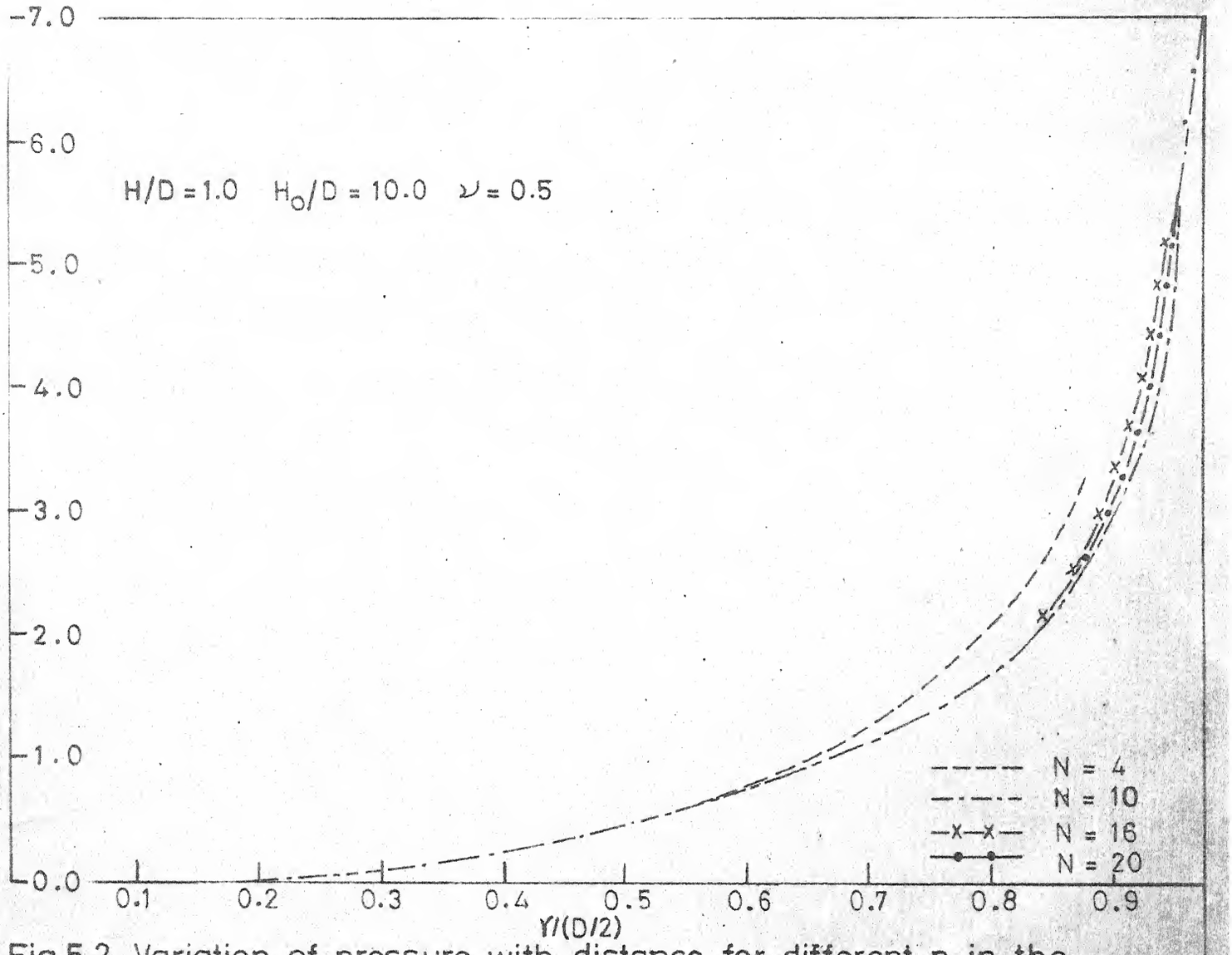

Fig.5.2 Variation of pressure with distance for different n in the analysis of vane mechanism I-strips

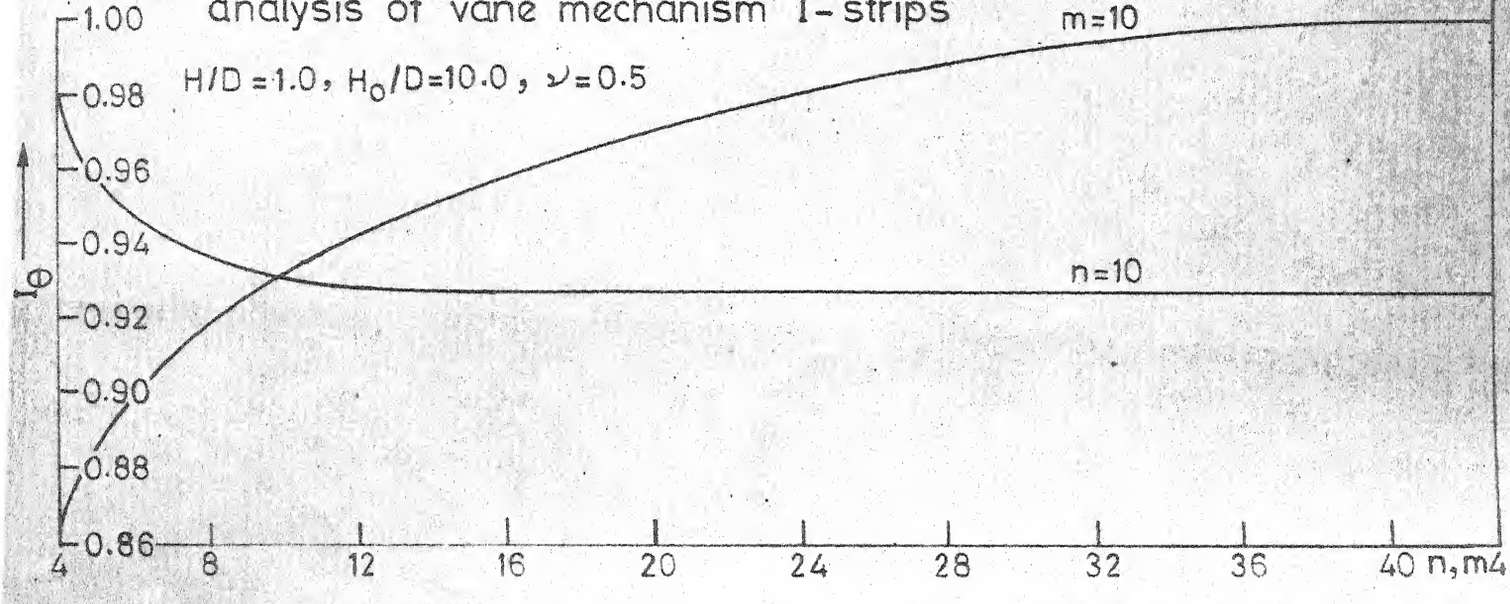

Fig.5.1 Variation of I_θ with n and m in the analysis mechanism I - strips

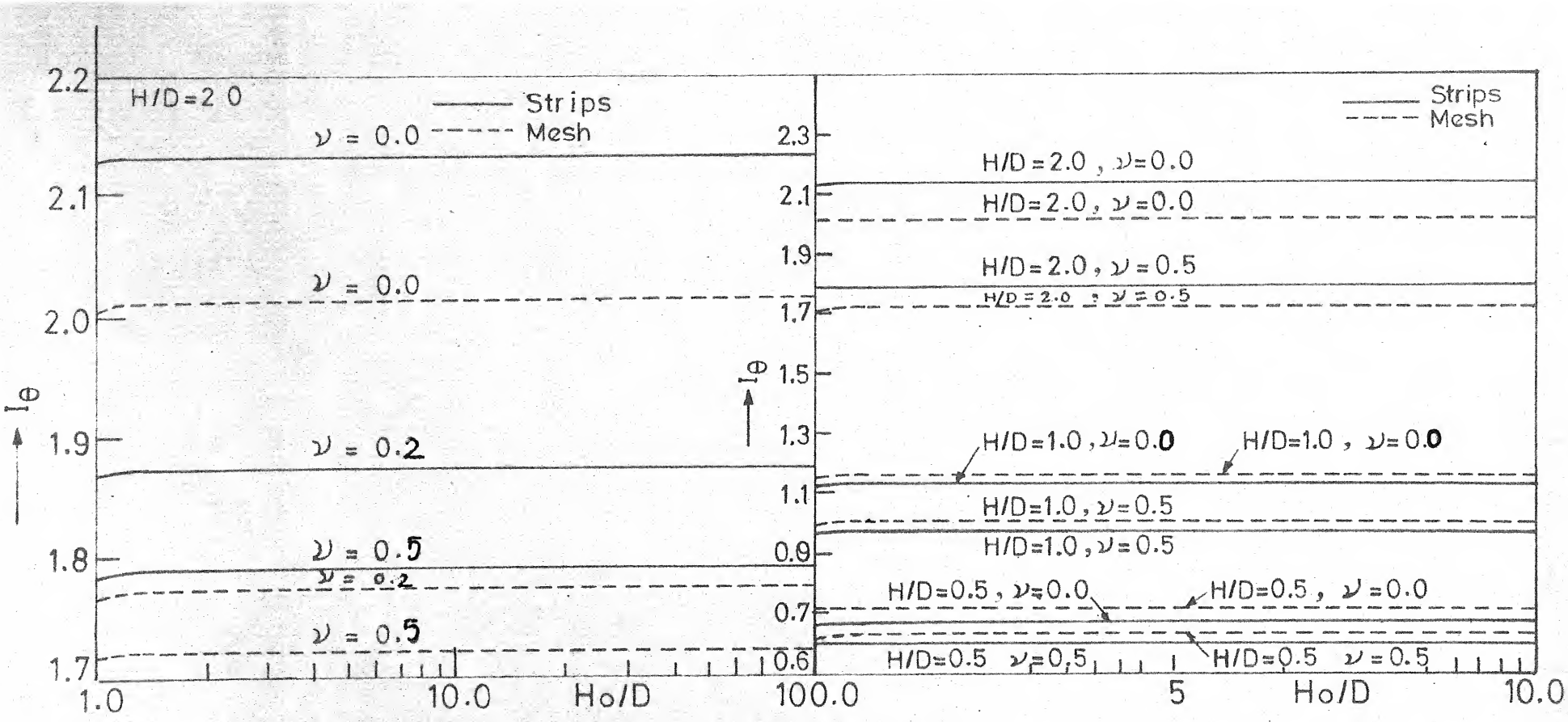

Fig. 5.3 (a) Variation of I_θ with Ho/D for various values of ν-mechanism I

Fig. 5.3 (b) Variation of I_θ with Ho/D for various values of H /D-mechanism I

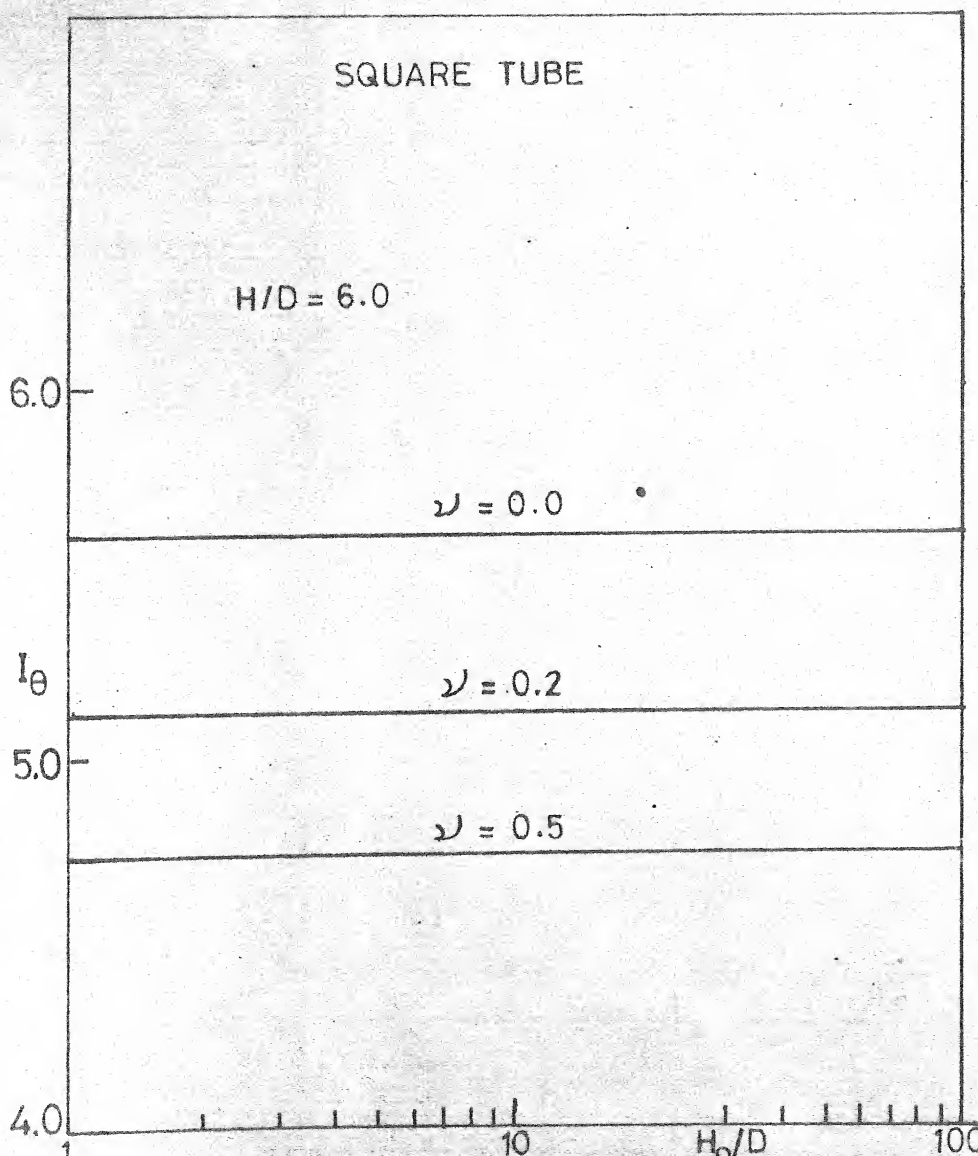

Fig.5.4a Variation of I_θ with H_o/D for various values of ν

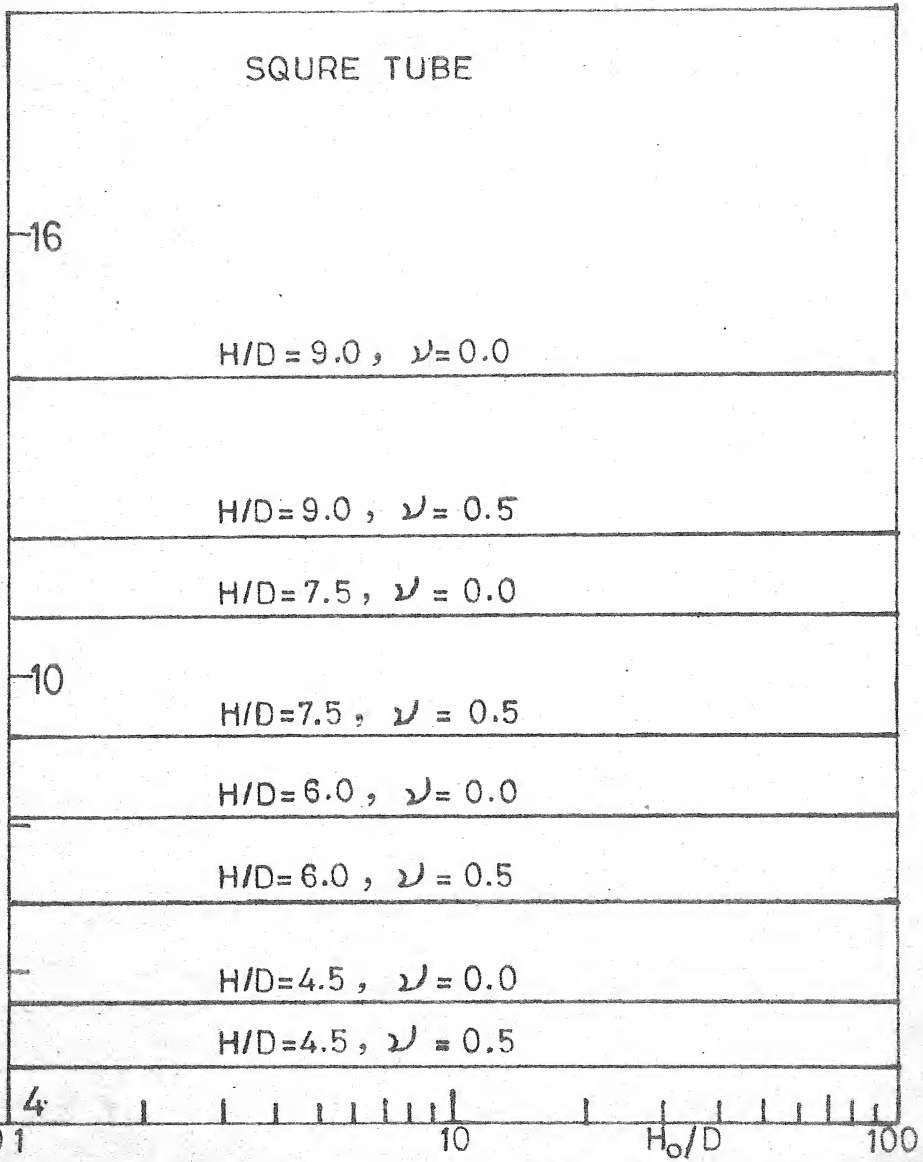

Fig.5.4b Variation of I_θ with H_o/D for various values of H/D

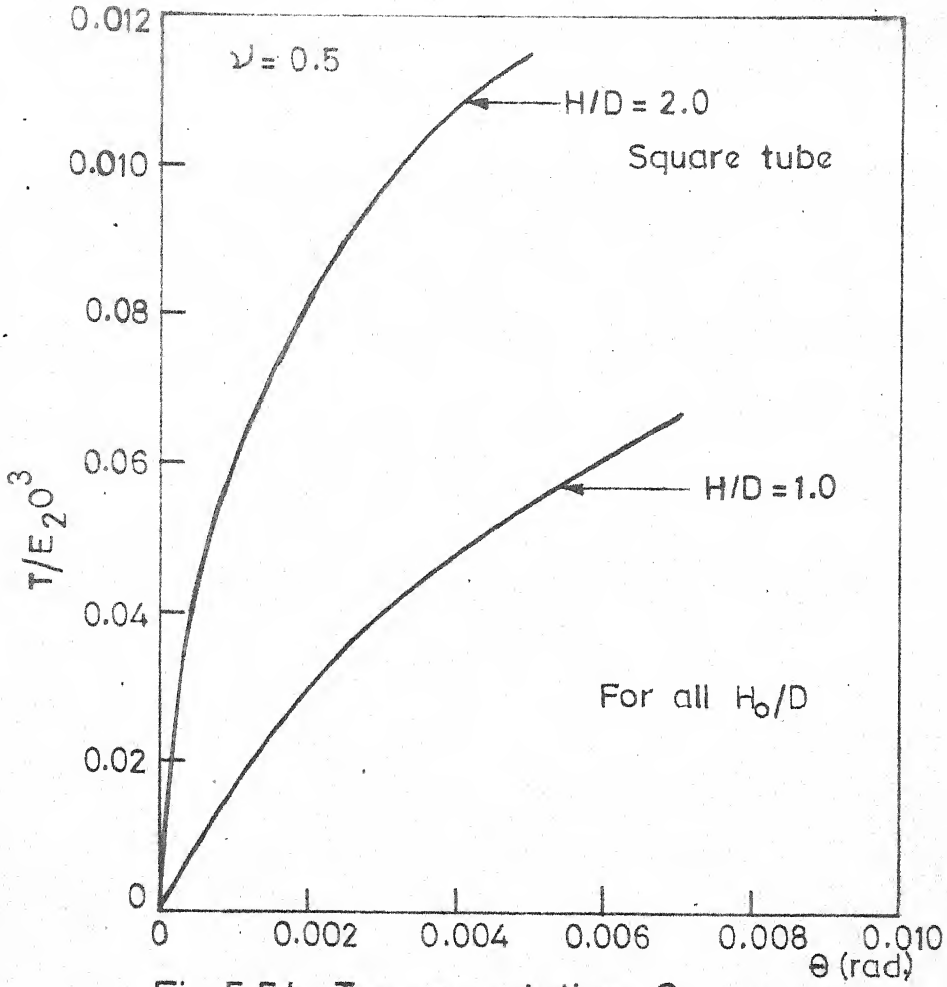

Fig.5.5 b Torque-rotation θ curves

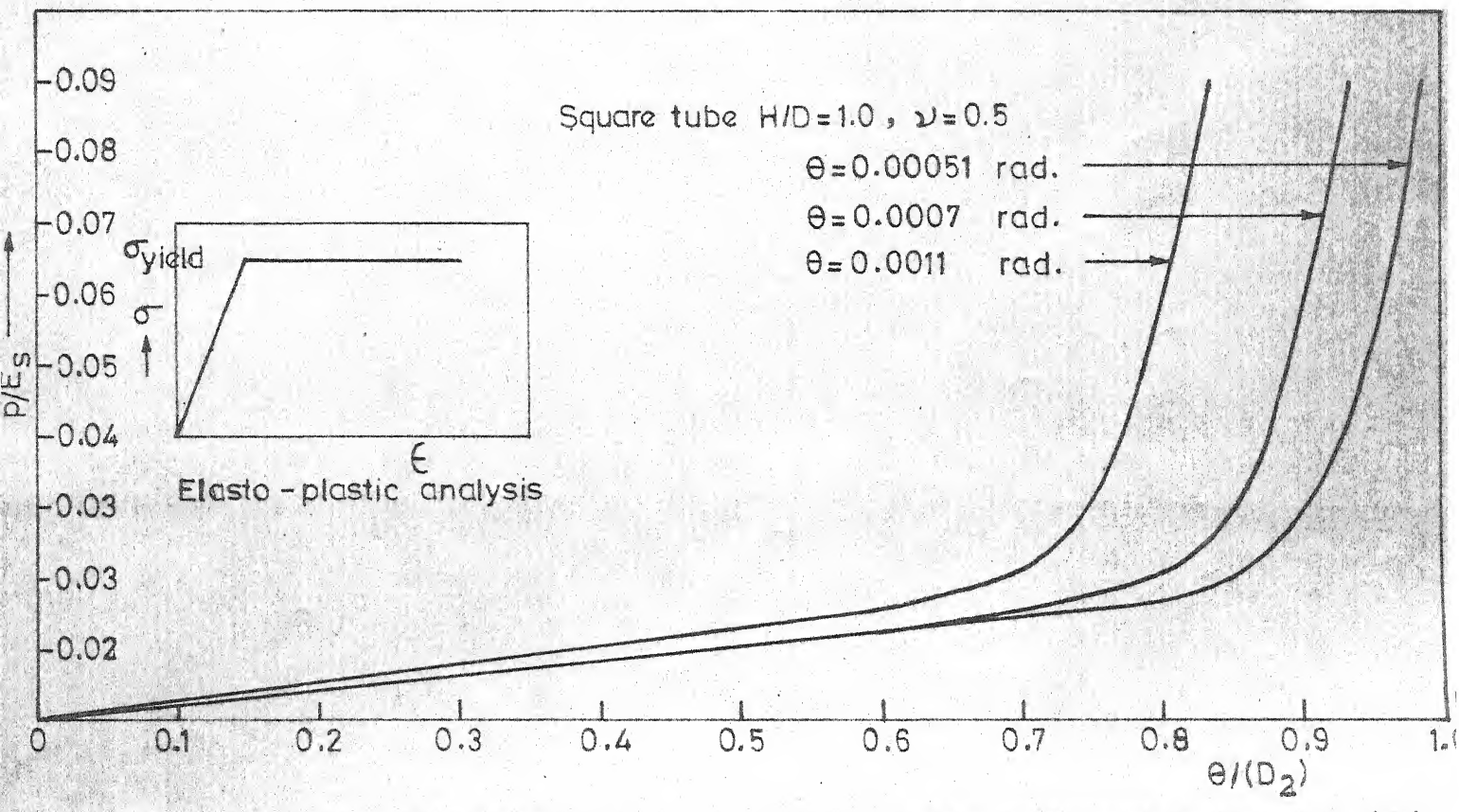

Fig.5.5 a Variation of pressure with distance for different rotations (θ)

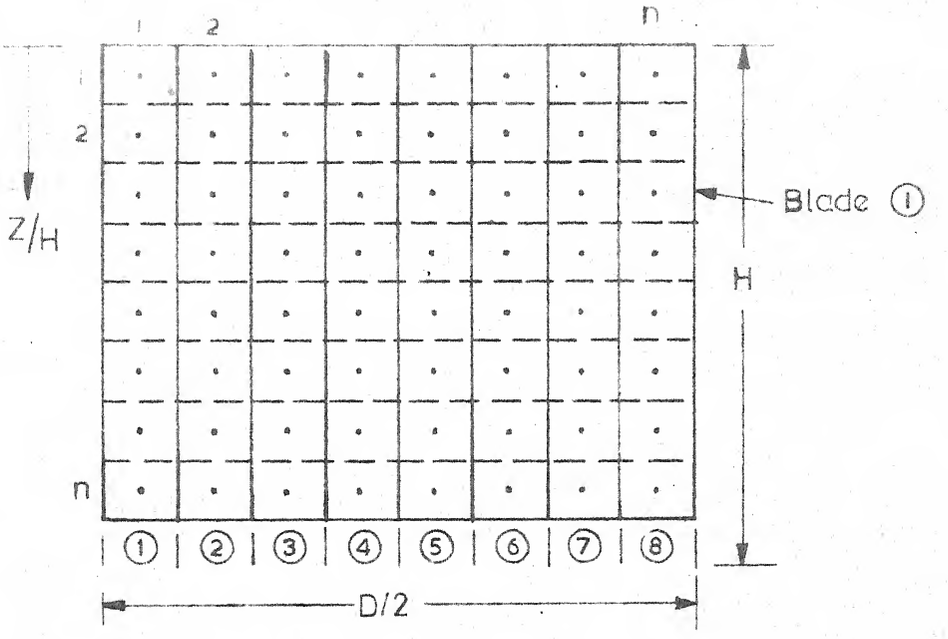

(a) Mechanism I-mesh

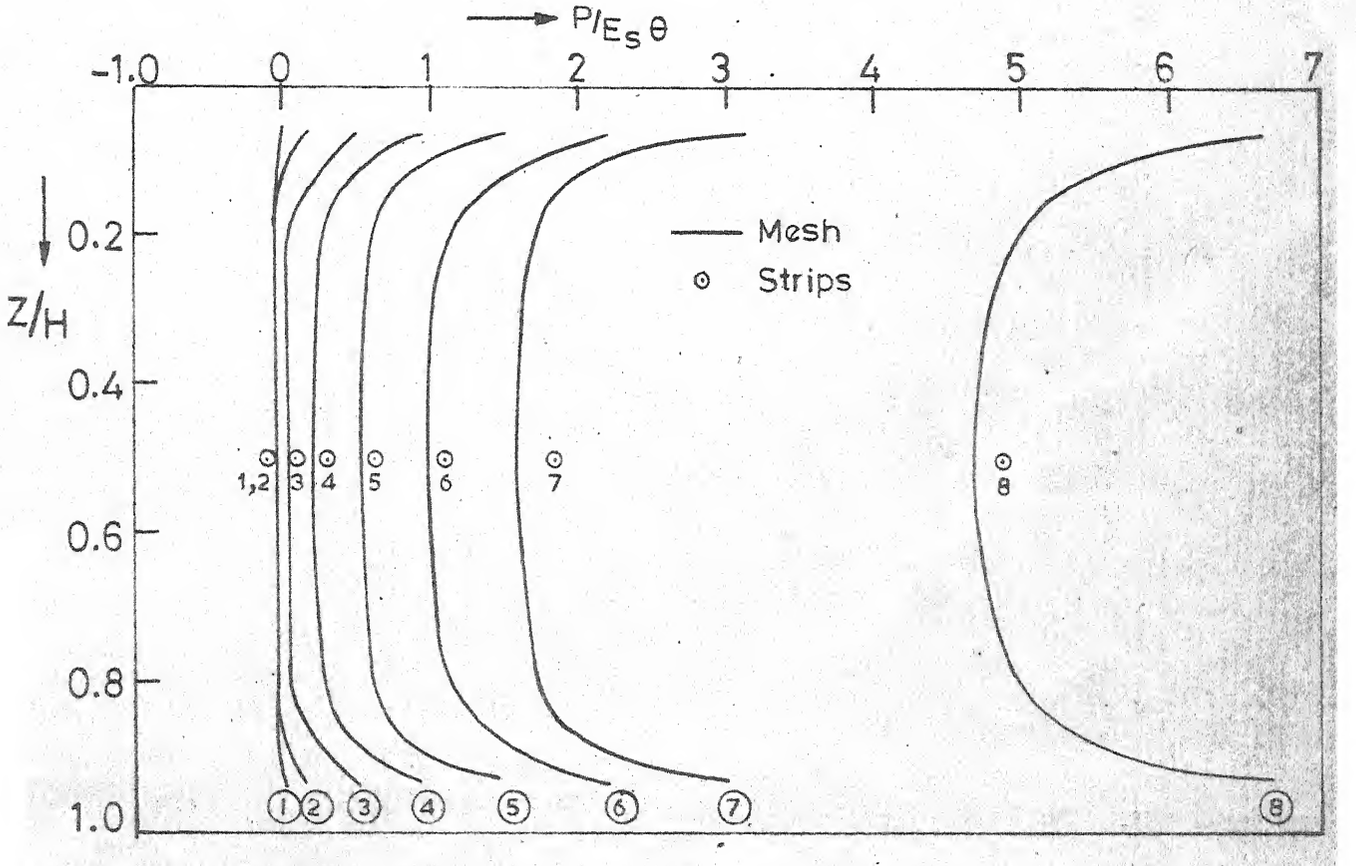

(b) Variation pressure with depth of the vane blade

Fig. 5.6 Comparison of pressures from mesh and strips-mechanism. I

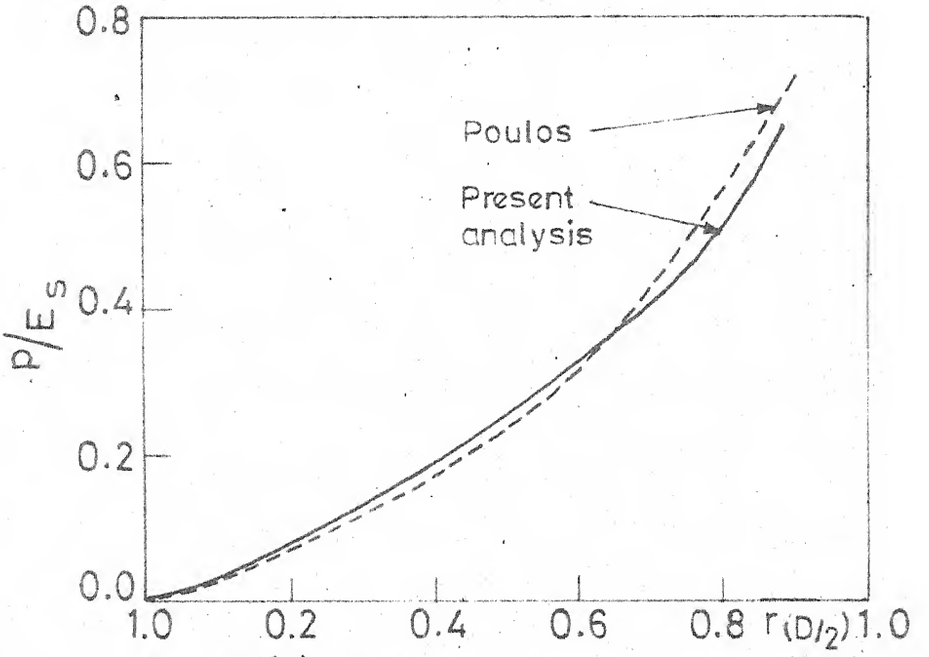

Fig.5.7(a) Variation of pressure with distance on bottom surface of the cylinder

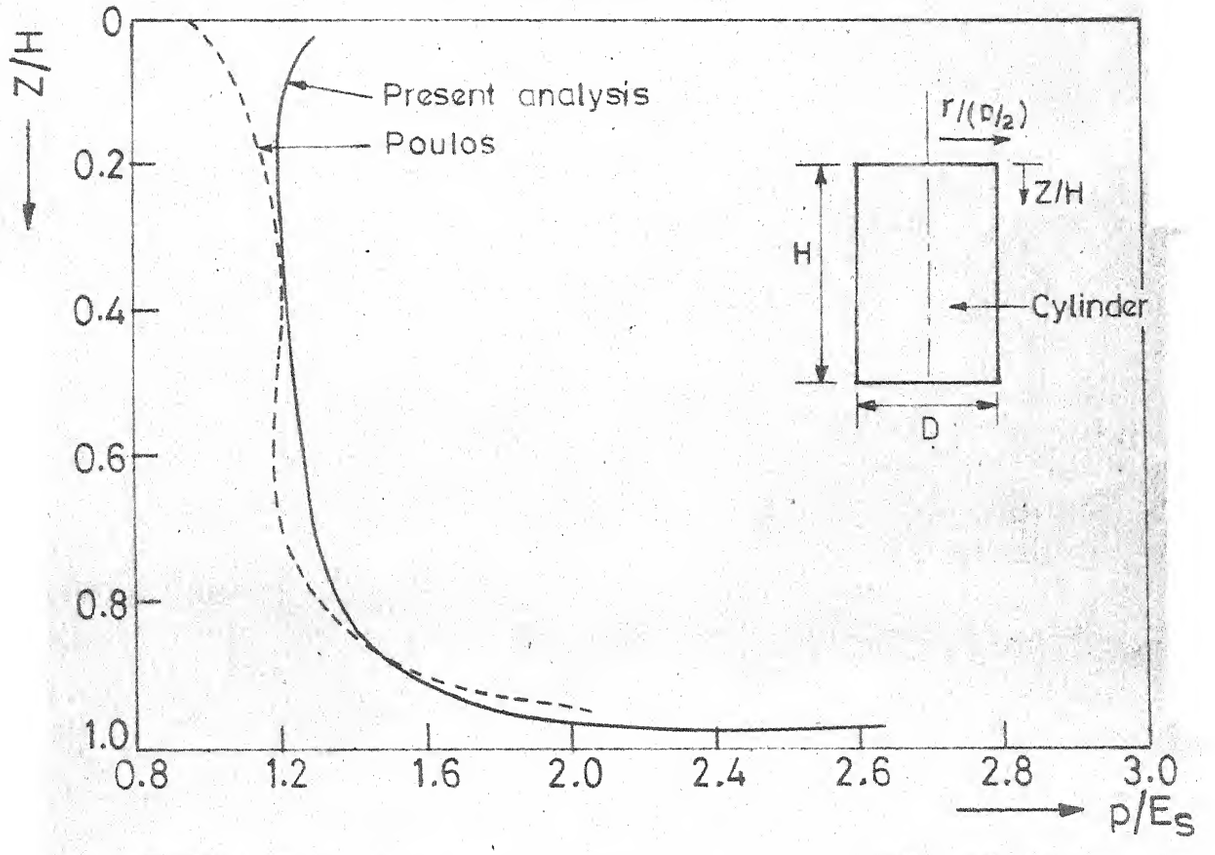

Fig.5.7(b) Variation of pressure with depth of the cylinder

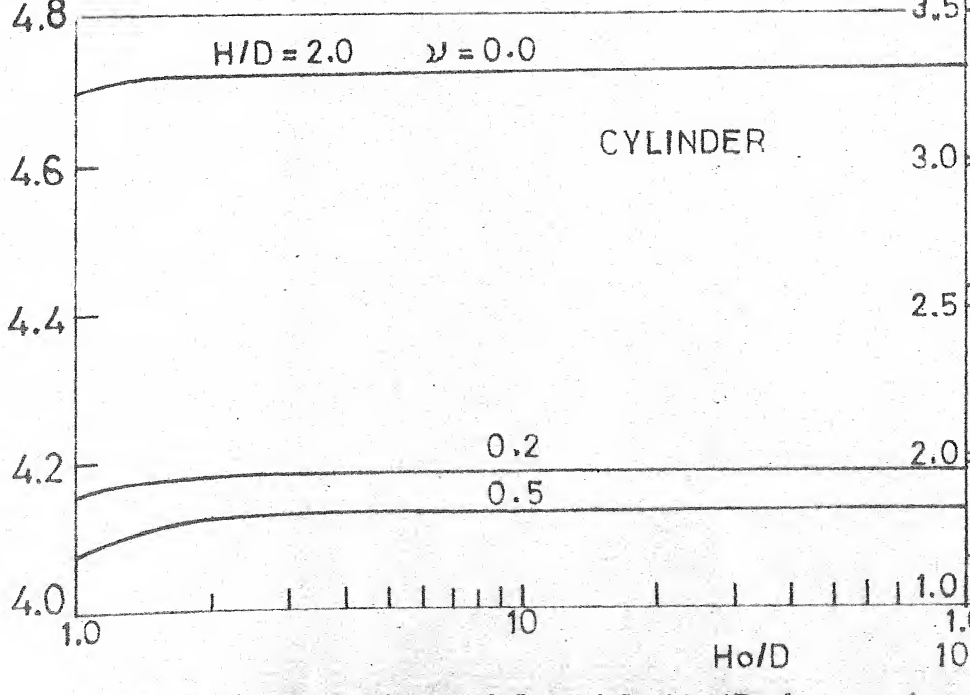

Fig.5.8(a) Variation of I_0 with Ho/D for various values of ν, mechanism II

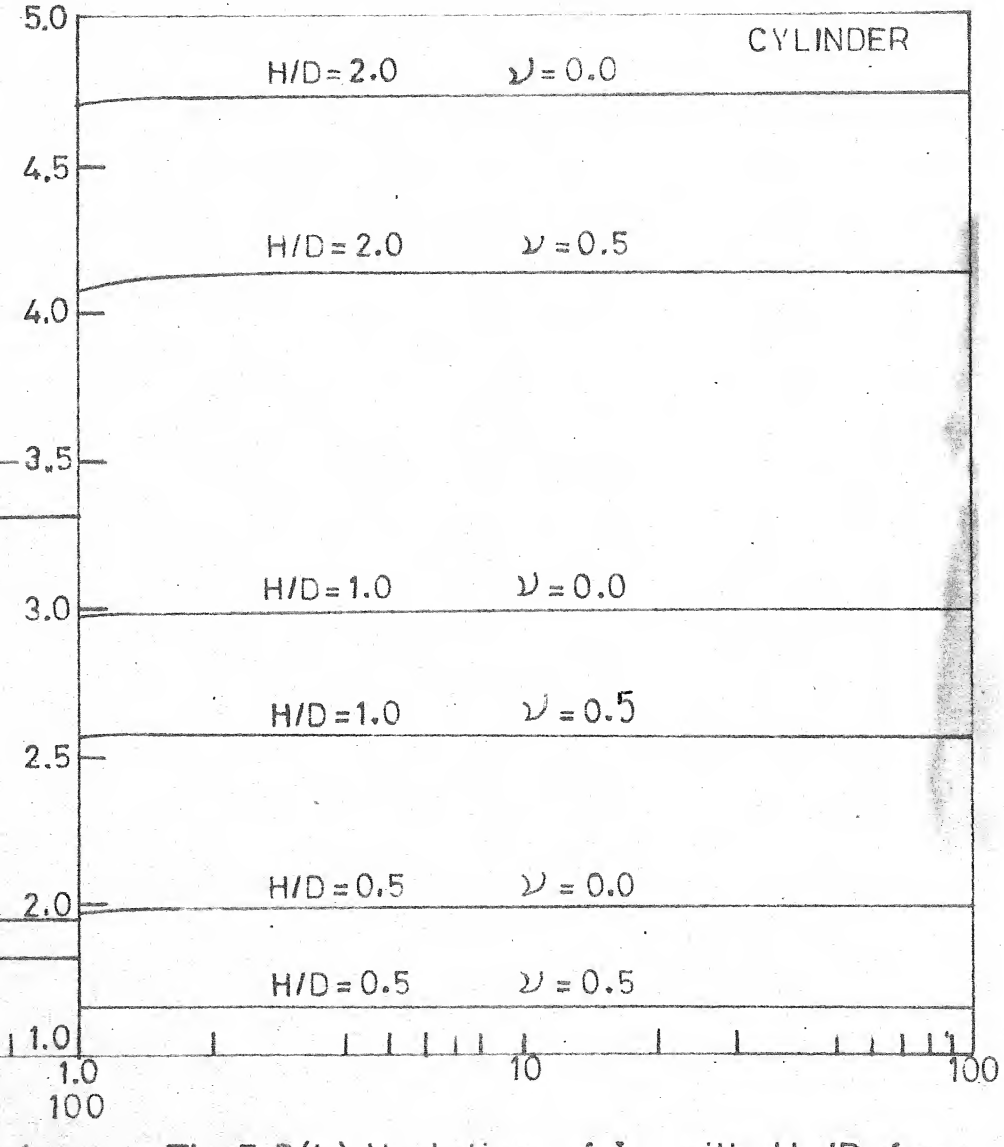

Fig.5.8(b) Variation of I_0 with Ho/D for various values of ν, mechanism II